

DAFTAR PUSTAKA

- Abdulnabi, Z.A., Al-doghachi, F.A.J., and Abdulsahib, H.T., 2021, Synthesis, characterization and thermogravimetric study of some metal complexes of selenazone ligand nanoparticles analogue of dithizone, *Indonesian J. Chem.*, 21, 1231–1243.
- Aminy, D.E., Rusdiarso, B., and Mudasir, M., 2022, Adsorption of Cd(II) ion from the solution using selective adsorbent of dithizone-modified commercial bentonite, *Int. J. Environ. Sci. Technol.*, 19, 6399–6410.
- Amiri, Z., Malmir, M., Hosseinejad, T., Kafshdarzadeh, K., and Heravi, M.M., 2022, Combined experimental and computational study on Ag-NPs immobilized on rod-like hydroxyapatite for promoting Hantzsch reaction, *Mol. Catal.*, 524, 112319.
- Angotzi, M.S., Mamei, V., Zákutná, D., Rusta, N., and Cannas, C., 2023, On the thermal and hydrothermal stability of spinel iron oxide nanoparticles as single and core-shell hard-soft phases, *J. Alloys Compd.*, 940, 168909.
- Anonim, 2017, Standar baku mutu kesehatan lingkungan dan persyaratan kesehatan air untuk keperluan higiene sanitasi, kolam renang, solus per aqua, dan pemandian umum, Jakarta.
- Appannagari, R.R., 2017, Environmental pollution causes and consequences: a study, *N. Asian Int. Res. J. Soc. Sci. Humanit.*, 3, 151–161.
- Avci, A., İnci, İ., and Baylan, N., 2019, A comparative adsorption study with various adsorbents for the removal of ciprofloxacin hydrochloride from water, *Water Air Soil Pollut.*, 230, 1–9.
- Benzaoui, T., Selatnia, A., and Djabali, D., 2018, Adsorption of copper (II) ions from aqueous solution using bottom ash of expired drugs incineration, *Adsorp. Sci. Technol.*, 36, 114–129.
- Bhatt, A., Priyadarshini, S., Mohanakrishnan, A.A., Abri, A., Sattler, M., and Techapaphawit, S., 2019, Physical, chemical, and geotechnical properties of coal fly ash: A global review, *Case Stud. Constr. Mater.*, 11, e00263.
- Chen, X., Zhang, G., Li, J., and Ji, P., 2021, Possibility of removing Pb and Cd from polluted water by modified fly ash, *Adsorp. Sci. Technol.*, 2021, 1-8.
- Chen, Y., Li, B., Ouyang, S., and Zhang, Y., 2019, Preparation of Fe-diopside matrix composites from iron tailings and fly ash, *IOP Conf. Ser. Mater. Sci. Eng.*, 678, 12103.
- Chen, Z., Song, G., Li, C., Chen, W., Li, Z., and Kawi, S., 2023, Coal fly ash to Y zeolite of great purity and crystallinity: A new and green activation method of combined in situ microwave and ultrasound, *Solid State Sci.*, 136, 107102.
- Cheng, S., Liu, Y., Xing, B., Qin, X., Zhang, C., and Xia, H., 2021, Lead and

- cadmium clean removal from wastewater by sustainable biochar derived from poplar saw dust, *J. Cleaner Prod.*, 314, 128074.
- Dodrill, B. and Lindemuth, J.R., 2021, Vibrating sample magnetometry, *Magnetochem. Mater. Charact.*, 15–37.
- Dou, X., Dai, H., Skuza, L., and Wei, S., 2022, Cadmium removal potential of hyperaccumulator *solanum nigrum* L. under two planting modes in three years continuous phytoremediation, *Environ. Pollut.*, 307, 119493.
- El-Eswed, B.I., 2020, Chemical evaluation of immobilization of wastes containing Pb, Cd, Cu and Zn in alkali-activated materials: A critical review, *J. Environ. Chem. Eng.*, 8, 104194.
- Fan, C., Wang, B., Ai, H., Qi, Y., and Liu, Z., 2021, A comparative study on solidification/stabilization characteristics of coal fly ash-based geopolymer and portland cement on heavy metals in MSWI fly ash, *J. Cleaner Prod.*, 319, 128790.
- Faradilla, F.S., Nugroho, D.T., Hidayati, R.E., Bayuaji, R., Hartanto, D., and Fansuri, H., 2020, Optimization of SiO₂/Al₂O₃ ratio in the preparation of geopolymer from high calcium fly ash, *IOP Conf. Ser. Earth Environ.*, 616, 12051.
- Feng, C., Huang, M., and Huang, C., 2023, Specific chemical adsorption of selected divalent heavy metal ions onto hydrous γ -Fe₂O₃-biochar from dilute aqueous solutions with pH as a master variable, *Chem. Eng. J.*, 451, 138921.
- Fernández-Jiménez, A., Garcia-Lodeiro, I., Maltseva, O., and Palomo, A., 2019, Mechanical-chemical activation of coal fly ashes: An effective way for recycling and make cementitious materials, *Front. Mater.*, 6, 1–12.
- Fitriana, D., Mudasir, M., and Siswanta, D., 2020, Adsorption of Pb(II) from aqueous solutions on dithizone-immobilized coal fly ash, *Key Eng. Mater.*, 840, 57–63.
- Ganapathe, L.S., Mohamed, M.A., Mohamad Yunus, R., and Berhanuddin, D.D., 2020, Magnetite (Fe₃O₄) nanoparticles in biomedical application: From synthesis to surface functionalisation, *Magnetochem.*, 6, 68.
- Genchi, G., Sinicropi, M.S., Lauria, G., Carocci, A., and Catalano, A., 2020, The effects of cadmium toxicity, *Int. J. Environ. Res. Public Health.*, 17, 3782.
- Ghorbanzadeh, N., Abdulrahimi, S., Forghani, A., and Farhangi, M.B., 2020, Bioremediation of cadmium in a sandy and a clay soil by microbially induced calcium carbonate precipitation after one week incubation, *Arid Land Res. Manag.*, 34, 319–335.
- Gogoi, B. and Das, U., 2022, Structural, magnetic and thermal characteristic analysis of synthesized magnetite spinel ferrite nanoparticles, *Res. Square.*, 1, 1–20.
- Guo, C., Zhao, L., Yang, J., Wang, K., and Zou, J., 2020, A novel perspective

- process for alumina extraction from coal fly ash via potassium pyrosulfate calcination activation method, *J. Cleaner Prod.*, 271, 122703.
- Hamisu, A.M., Ariffin, A., and Wibowo, A.C., 2020, Cation exchange in metal-organic frameworks (MOFs): The hard-soft acid-base (HSAB) principle appraisal, *Inorg. Chim. Acta.*, 511, 119801.
- Han, D., Wu, X., Li, R., Tang, X., Xiao, S., and Scholz, M., 2021, Critical review of electro-kinetic remediation of contaminated soils and sediments: mechanisms, performances and technologies, *Water Air Soil Pollut.*, 232, 335.
- Harja, M., Buema, G., Lupu, N., Chiriac, H., Herea, D.D., and Ciobanu, G., 2020, Fly ash coated with magnetic materials: Improved adsorbent for Cu(II) removal from wastewater, *Mater.*, 14, 63.
- Harja, M., Lupu, N., Chiriac, H., Herea, D.D., and Buema, G., 2022, Studies on the removal of congo red dye by an adsorbent based on fly-ash@ Fe₃O₄ mixture, *Magnetochem.*, 8, 125.
- Hashim, K.S., Ewadh, H.M., Muhsin, A.A., Zubaidi, S.L., Kot, P., Muradov, M., Aljefery, M., and Al-Khaddar, R., 2021, Phosphate removal from water using bottom ash: Adsorption performance, coexisting anions and modelling studies, *Water Sci. Technol.*, 83, 77–89.
- Hockaday, J., Harvey, A., and Velasquez-Orta, S., 2022, A comparative analysis of the adsorption kinetics of Cu²⁺ and Cd²⁺ by the microalgae *Chlorella vulgaris* and *Scenedesmus obliquus*, *Algal Res.*, 64, 102710.
- Hong, S.H., Shin, M.C., Lee, J., Lee, C.G., Song, D.S., Um, B.H., and Park, S.J., 2021, Recycling of bottom ash derived from combustion of cattle manure and its adsorption behaviors for Cd(II), Cu(II), Pb(II), and Ni(II), *Environ. Sci. Pollut. Res.*, 28, 14957–14968.
- Hoyos-Montilla, A.A., Tobón, J.I., and Puertas, F., 2023, Role of calcium hydroxide in the alkaline activation of coal fly ash, *Cem. Concr. Compos.*, 137, 104925.
- Huang, X., Zhao, H., Hu, X., Liu, F., Wang, L., Zhao, X., Gao, P., and Ji, P., 2020, Optimization of preparation technology for modified coal fly ash and its adsorption properties for Cd²⁺, *J. Hazard. Mater.*, 392, 122461.
- Huang, X., Zhao, H., Zhang, G., Li, J., Yang, Y., and Ji, P., 2020, Potential of removing Cd(II) and Pb(II) from contaminated water using a newly modified fly ash, *Chemosphere*, 242, 125148.
- Huda, B.N., Wahyuni, E.T., and Mudasir, M., 2021, Eco-friendly immobilization of dithizone on coal bottom ash for the adsorption of lead(II) ion from water, *Results Eng.*, 10, 100221.
- Huda, B.N., Wahyuni, E.T., and Mudasir, M., 2022, Greener procedure of dithizone immobilization on coal bottom ash for heavy metal adsorbent: synthesis optimization and characterization, *Key Eng. Mater.*, 927, 3–10.

- Huda, B.N., Wahyuni, E.T., and Mudasir, M., 2023, Simultaneous adsorption of Pb (II) and Cd (II) in the presence of Mg(II) ion using eco-friendly immobilized dithizone on coal bottom ash, *S. Afr. J. Chem. Eng.*, 45, 315–327.
- Hussain, Z., Chang, N., Sun, J., Xiang, S., Ayaz, T., Zhang, H., and Wang, H., 2022, Modification of coal fly ash and its use as low-cost adsorbent for the removal of directive, acid and reactive dyes, *J. Hazard. Mater.*, 422, 126778.
- Javadian, H., Ghorbani, F., Tayebi, H.A., and Asl, S.M.H., 2015, Study of the adsorption of Cd(II) from aqueous solution using zeolite-based geopolymer, synthesized from coal fly ash; kinetic, isotherm and thermodynamic studies, *Arab. J. Chem.*, 8, 837–849.
- Joseph, I. V., Tosheva, L., and Doyle, A.M., 2020, Simultaneous removal of Cd(II), Co(II), Cu(II), Pb(II), and Zn(II) ions from aqueous solutions via adsorption on FAU-type zeolites prepared from coal fly ash, *J. Environ. Chem. Eng.* 8, 103895.
- Khaled, B., Wided, B., Béchir, H., Elimame, E., Mouna, L., and Zied, T., 2019, Investigation of electrocoagulation reactor design parameters effect on the removal of cadmium from synthetic and phosphate industrial wastewater, *Arab. J. Chem.*, 12, 18,48–1859.
- Koo, K.N., Ismail, A.F., Othman, M.H.D., Bidin, N., and Rahman, M.A., 2019, Preparation and characterization of superparamagnetic magnetite (Fe₃O₄) nanoparticles: A short review, *Malaysian J. Fundam. Appl. Sci.*, 15, 23–31.
- Krishnamoorthy, S., Ajala, F., Mohammed, S.M., Asok, A., and Shukla, S., 2021, High adsorption and high catalyst regeneration kinetics observed for fly ash-Fe₃O₄-Ag magnetic composite for efficient removal of industrial azo reactive dyes from aqueous solution via persulfate activation, *Appl. Surf. Sci.*, 548, 149265.
- Kubier, A., Wilkin, R.T., and Pichler, T., 2019, Cadmium in soils and groundwater: a review, *Appl. Geochem.*, 108, 104388.
- Li, J., Wang, Y., Chen, Z., and Rahman, S.S., 2020, Simulation of adsorption–desorption behavior in coal seam gas reservoirs at the molecular level: a comprehensive review, *Energy Fuels.*, 34, 2619–2642.
- Li, L., Bi, R., Wang, Z., Xu, C., Li, B., Luan, L., Chen, X., Xue, F., Zhang, S., and Zhao, N., 2019, Speciation of mercury using high-performance liquid chromatography-inductively coupled plasma mass spectrometry following enrichment by dithizone functionalized magnetite-reduced graphene oxide, *Spectrochim. Acta B: At. Spectrosc.*, 159, 105653.
- Luo, Y., Wu, Y.H., Ma, S.H., Zheng, S.L., and Chu, P.K., 2019, An eco-friendly and cleaner process for preparing architectural ceramics from coal fly ash: Pre-activation of coal fly ash by a mechanochemical method, *J. Cleaner Prod.*, 214, 419–428.

- Mabuza, M., Premllal, K., and Daramola, M.O., 2022, Modelling and thermodynamic properties of pure CO₂ and flue gas sorption data on south african coals using langmuir, freundlich, temkin, and extended langmuir isotherm models, *Int. J. Coal Sci. Technol.*, 9, 45.
- Manjuladevi, M., Anitha, R., and Manonmani, S., 2018, Kinetic study on adsorption of Cr(VI), Ni(II), Cd(II) and Pb(II) ions from aqueous solutions using activated carbon prepared from cucumis melo peel, *Appl. Water Sci.*, 8, 1–8.
- Miranda, G., Wahyuni, E.T., and Mudasir, M., 2022, Immobilization of dithizone on coal fly ash in alkaline medium as adsorbent of Cd(II) ion, *Key Eng. Mater.*, 927, 11–19.
- Mudasir, M., Baskara, R.A., Suratman, A., Yunita, K.S., Perdana, R., and Puspitasari, W., 2020, Simultaneous adsorption of Zn(II) and Hg(II) ions on selective adsorbent of dithizone-immobilized bentonite in the presence of Mg (II) ion, *J. Environ. Chem. Eng.*, 8, 104002.
- Mushtaq, F., Zahid, M., Bhatti, I.A., Nasir, S., and Hussain, T., 2019, Possible applications of coal fly ash in wastewater treatment, *J. Environ. Manage.*, 240, 27–46.
- do Nascimento, F.H. and Masini, J.C., 2023, Porous polymer monolith decorated with dithizone for greener visual and spectrophotometric sensing of Hg (II), *Sens. Actuators B Chem.*, 381, 133385.
- Pandey, R., Kumar, A., Xu, Q., and Pandey, D.S., 2020, Zinc (II), copper (II) and cadmium (II) complexes as fluorescent chemosensors for cations, *Dalton Trans.*, 49, 542–568.
- Patel, H., 2021, Review on solvent desorption study from exhausted adsorbent, *J. Saudi Chem. Soc.*, 25, 101302.
- Peng, Z., Lin, X., Zhang, Y., Hu, Z., Yang, X., Chen, C., Chen, H., Li, Y., and Wang, J., 2021, Removal of cadmium from wastewater by magnetic zeolite synthesized from natural, low-grade molybdenum, *Sci. Total Environ.*, 772, 145355.
- Rabaeh, K. and Basfar, A., 2020, Optical evaluation of dithizone solution as a new radiochromic dosimeter, *Pigment Resin Technol.*, 49, 249–253.
- Rajendran, S., Priya, A.K., Kumar, P.S., Hoang, T.K.A., Sekar, K., Chong, K.Y., Khoo, K.S., Ng, H.S., and Show, P.L., 2022, A critical and recent developments on adsorption technique for removal of heavy metals from wastewater-A review, *Chemosphere*, 303, 135146.
- Revellame, E.D., Fortela, D.L., Sharp, W., Hernandez, R., and Zappi, M.E., 2020, Adsorption kinetic modeling using pseudo-first order and pseudo-second order rate laws: A review, *Cleaner Eng. Technol.*, 1, 100032.
- Rodchom, M., Wimuktiwan, P., Soongprasit, K., Atong, D., and Vichaphund, S., 2022, Preparation and characterization of ceramic materials with low

- thermal conductivity and high strength using high-calcium fly ash, *International J. Miner. Metall. Mater.*, 29, 1635–1645.
- Santikulthani, S., Eknapakul, T., Pinitsoontorn, S., and Songsiriritthigul, P., 2023, Systematic investigation and correction of the magnetic hysteresis obtained by vibrating sample magnetometry, *J. Phys. Conf. Ser.*, 12058.
- Schöttner, L., Nefedov, A., Yang, C., Heissler, S., Wang, Y., and Wöll, C., 2019, Structural evolution of α -Fe₂O₃ (0001) surfaces under reduction conditions monitored by infrared spectroscopy, *Front. Chem.*, 7, 451.
- Sedghi, R., Heidari, B., Javadi, H., and Sayyari, N., 2022, Design and synthesis of colorimetric sensor based on dithizone@ TiO₂/poly (tert-butyl acrylate-acrylic acid) nanocomposite for fast visual detection of mercury, lead and cadmium ions in aqueous media, *Environ. Nanotechnol. Monit. Manage.*, 18, 100670.
- Sharma, G. and Naushad, M., 2020, Adsorptive removal of noxious cadmium ions from aqueous medium using activated carbon/zirconium oxide composite: isotherm and kinetic modelling, *J. Mol. Liq.*, 310, 113025.
- Singh, N.B., Agarwal, A., De, A., and Singh, P., 2022, Coal fly ash: An emerging material for water remediation, *Int. J. Coal Sci. Technol.*, 9, 44.
- Taha, G.M., Rashed, M.N., El-Sadek, M.S.A., and Moghazy, M.A.E., 2021, Multiferroic BiFeO₃ dithizone functionalized as optical sensor for detection and determination of some heavy metals in environmental samples, *Bull. Mater. Sci.*, 44, 122.
- Tighadouini, S., Radi, S., Ferbinteanu, M., and Garcia, Y., 2019, Highly selective removal of Pb(II) by a pyridylpyrazole- β -ketoenol receptor covalently bonded onto the silica surface, *ACS omega*, 4, 3954–3964.
- Ukaogo, P.O., Ewuzie, U., and Onwuka, C.V, 2020, Environmental pollution: causes, effects, and the remedies, *Microorganisms Sustain. Environ. Health.*, 21, 419–429.
- Umejuru, E.C., Prabakaran, E., and Pillay, K., 2020, Coal fly ash coated with carbon hybrid nanocomposite for remediation of cadmium(II) and photocatalytic application of the spent adsorbent for reuse, *Results Mater.*, 7, 100117.
- Usman, U.A., Yusoff, I., Raoov, M., and Hodgkinson, J., 2019, The economic potential of the African iron-ore tailings: synthesis of magnetite for the removal of trace metals in groundwater-a review, *Environ. Earth Sci.*, 78, 1–22.
- Vardhan, K.H., Kumar, P.S., and Panda, R.C., 2019, A review on heavy metal pollution, toxicity and remedial measures: Current trends and future perspectives, *J. Mol. Liq.*, 290, 111197.
- Wang, C., Leng, S., Guo, H., Cao, L., and Huang, J., 2019, Acid and alkali treatments for regulation of hydrophilicity/hydrophobicity of natural zeolite, *Appl. Surf. Sci.*, 478, 319–326.

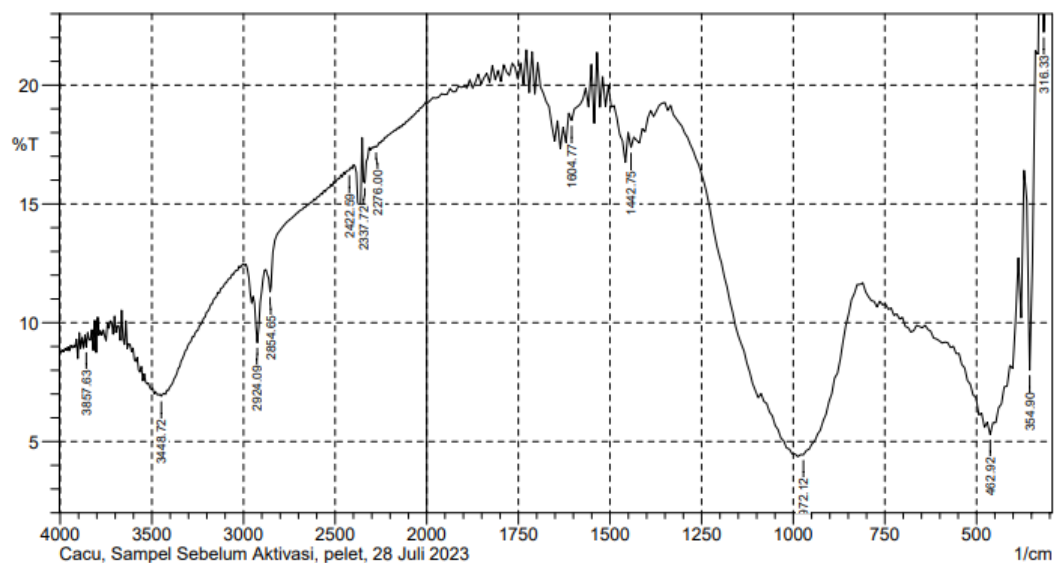
- Wang, J. and Guo, X., 2020, Adsorption isotherm models: Classification, physical meaning, application and solving method, *Chemosphere*, 258, 127279.
- Wang, T., Jiang, M., Yu, X., Niu, N., and Chen, L., 2022, Application of lignin adsorbent in wastewater treatment: A review, *Sep. Purif. Technol.*, 302, 122116.
- Xin, F., Xiao, R., Zhao, Y., and Zhang, J., 2022, Surface sulfidation modification of magnetospheres from fly ash for elemental mercury removal from coal combustion flue gas, *Chem. Eng. J.*, 436, 135212.
- Yang, L., Li, D., Zhu, Z., Xu, M., Yan, X., and Zhang, H., 2019, Effect of the intensification of preconditioning on the separation of unburned carbon from coal fly ash, *Fuel*, 242, 174–183.
- Zhang, J., Li, S., Li, H., Wu, Q., Xi, X., and Li, Z., 2017, Preparation of Al–Si composite from high-alumina coal fly ash by mechanical–chemical synergistic activation, *Ceram. Int.*, 43, 6532–6541.
- Zhang, M., Mao, Y., Wang, W., Yang, S., Song, Z., and Zhao, X., 2016, Coal fly ash/CoFe₂O₄ composites: a magnetic adsorbent for the removal of malachite green from aqueous solution, *RSC Adv.*, 6, 93564–93574.
- Zhao, H., Huang, X., Zhang, G., Li, J., He, Z., Ji, P., and Zhao, J., 2020, Possibility of removing cadmium pollution from the environment using a newly synthesized material coal fly ash, *Environ. Sci. Pollut. Res.*, 27, 4997–5008.
- Zhao, X., Zhao, H., Huang, X., Wang, L., Liu, F., Hu, X., Li, J., Zhang, G., and Ji, P., 2021, Effect and mechanisms of synthesis conditions on the cadmium adsorption capacity of modified fly ash, *Ecotoxicol. Environ. Saf.*, 223, 112550.
- Zhao, Y., Luan, H., Yang, B., Li, Z., Song, M., Li, B., and Tang, X., 2023, Adsorption of Pb, Cu and Cd from water on coal fly ash-red mud modified composite material: Characterization and mechanism, *Water (Switz.)*, 15, 767.

LAMPIRAN

Lampiran 1 Spektra FTIR ALB



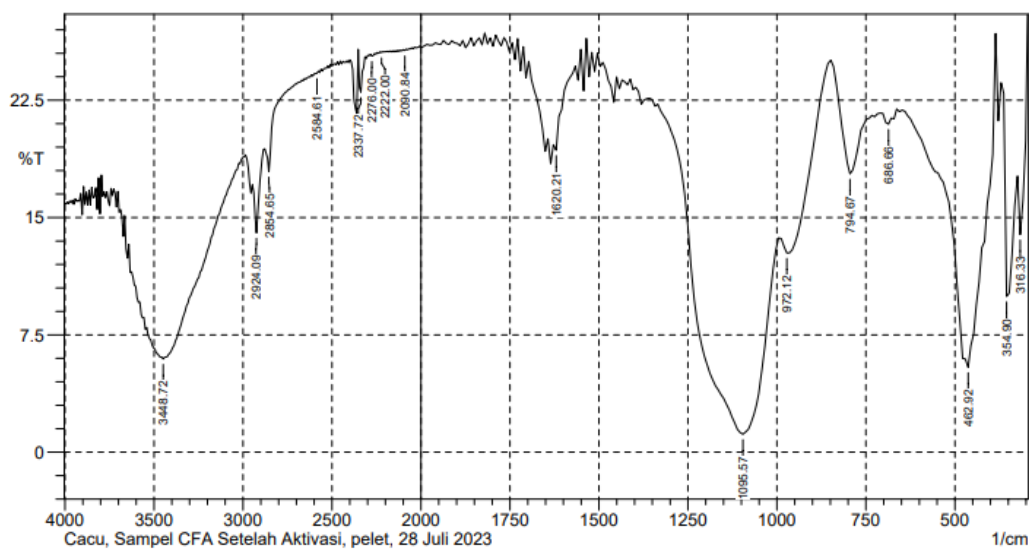
Lab. Kimia Organik FMIPA UGM



Lampiran 2 Spektra FTIR ALB-Akt



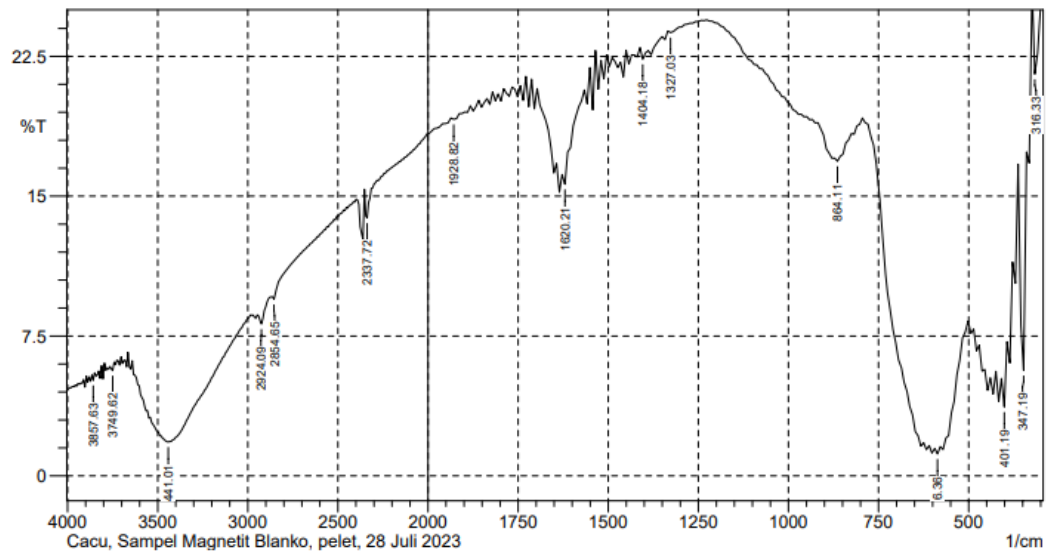
Lab. Kimia Organik FMIPA UGM



Lampiran 3 Spektra FTIR Fe_3O_4



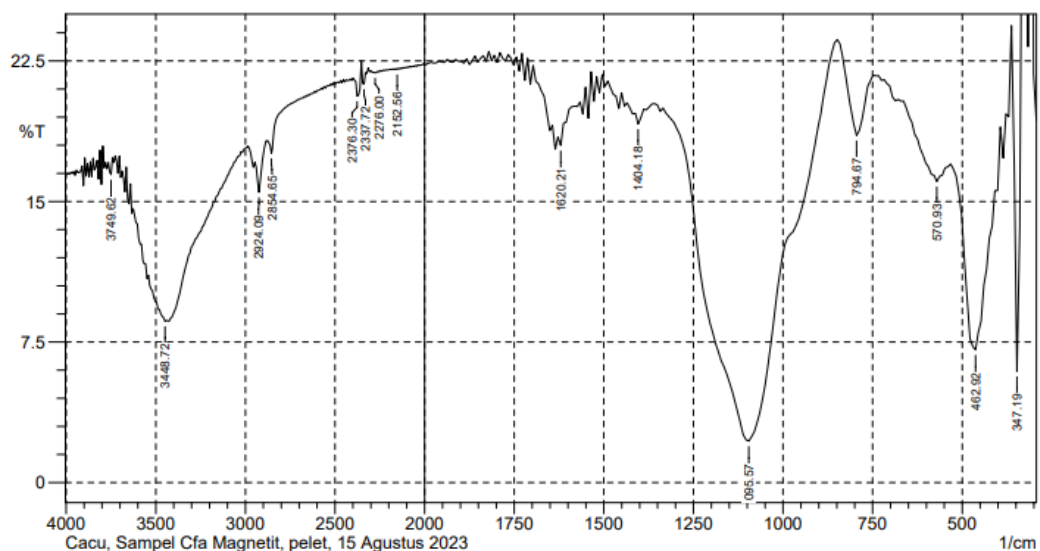
Lab. Kimia Organik FMIPA UGM



Lampiran 4 Spektra FTIR ALBM



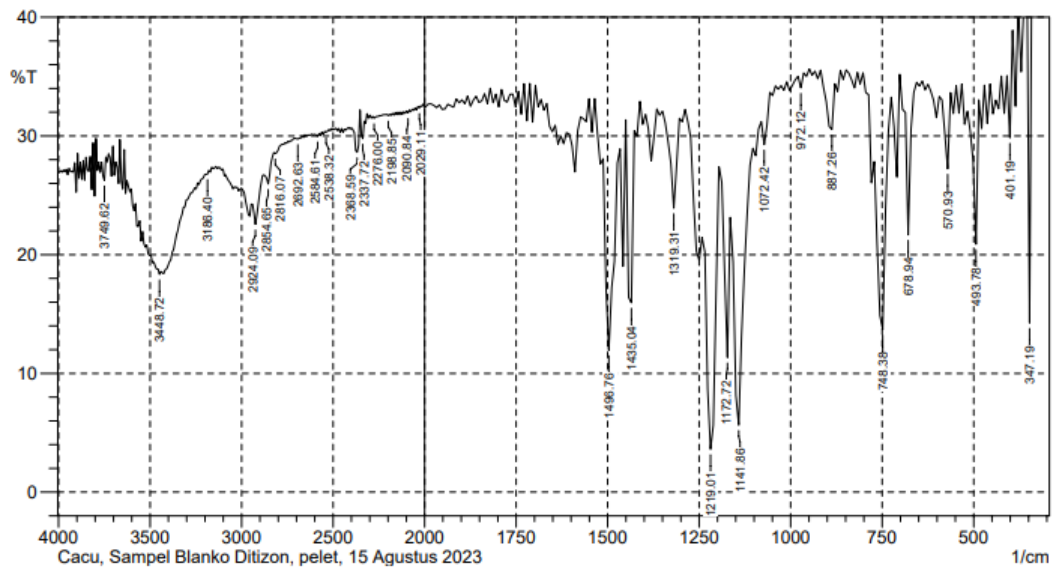
Lab. Kimia Organik FMIPA UGM



Lampiran 5 Spektra FTIR ditizon



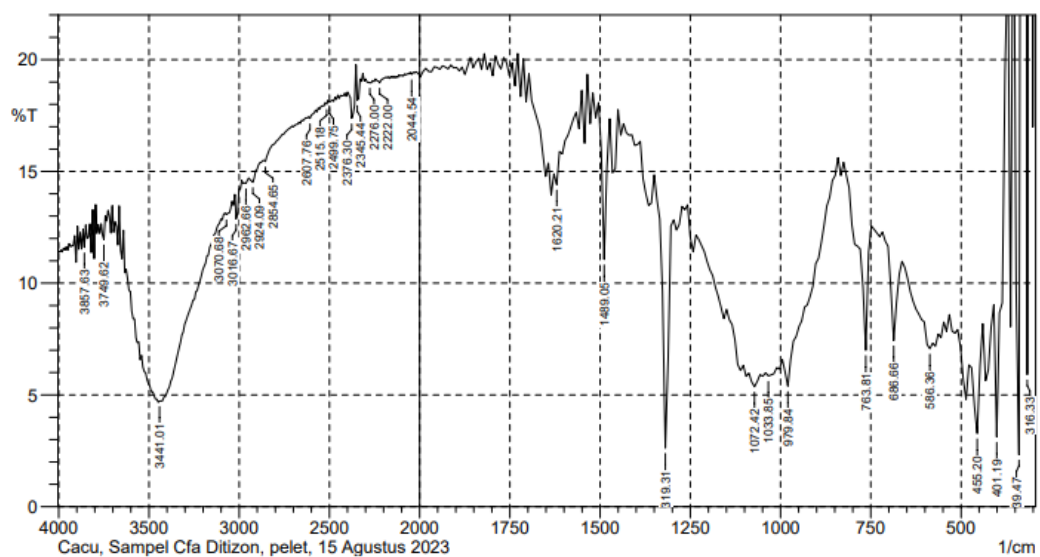
Lab. Kimia Organik FMIPA UGM



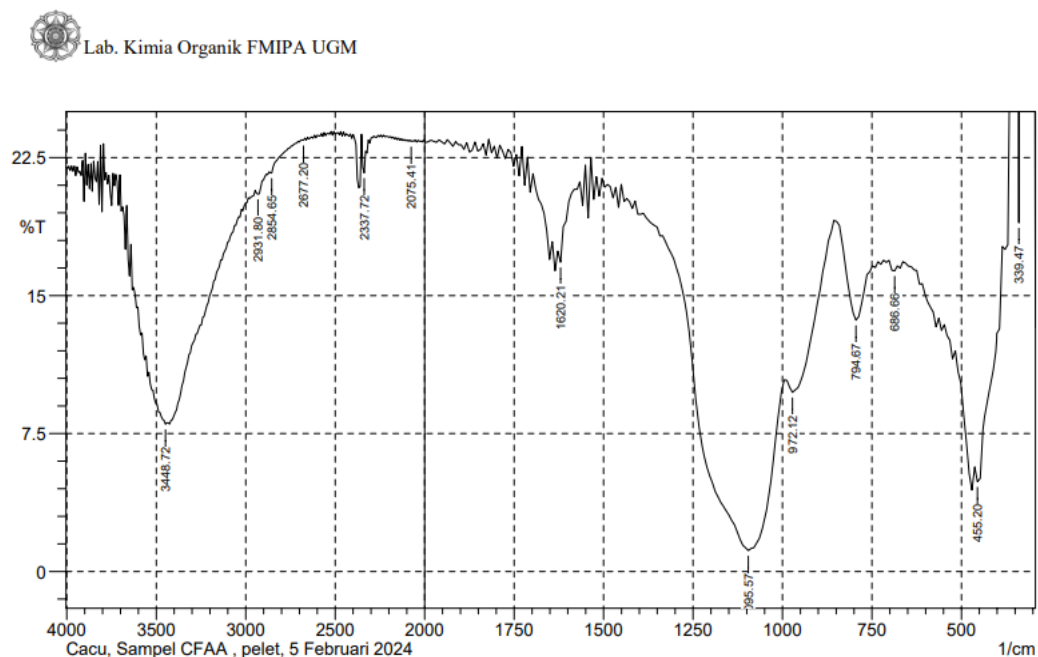
Lampiran 6 Spektra FTIR ALBM-Dtz



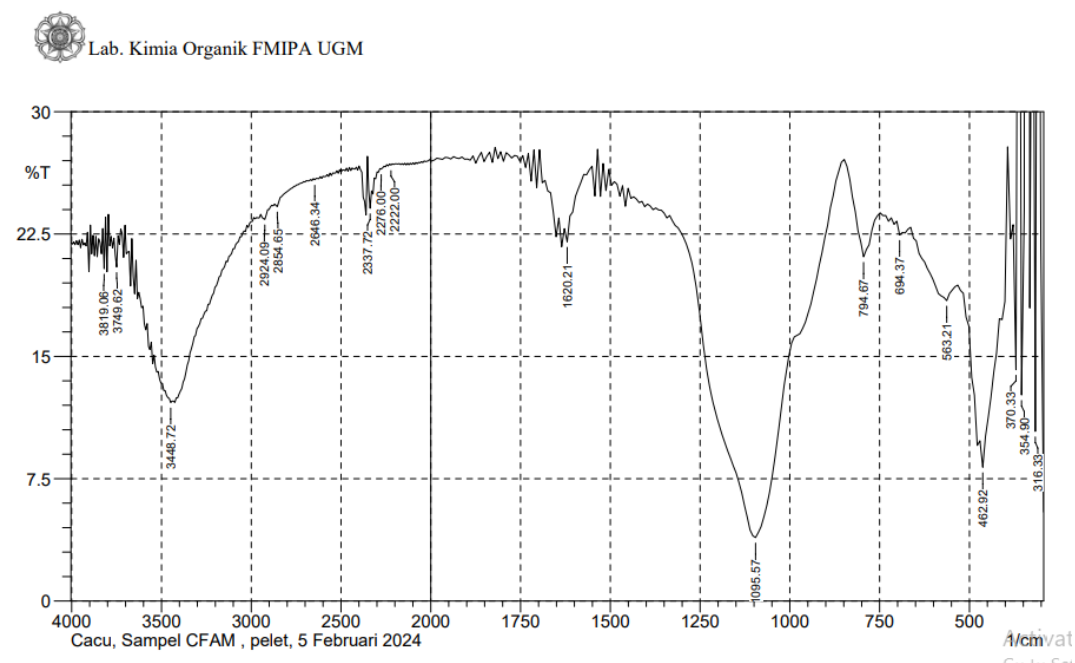
Lab. Kimia Organik FMIPA UGM



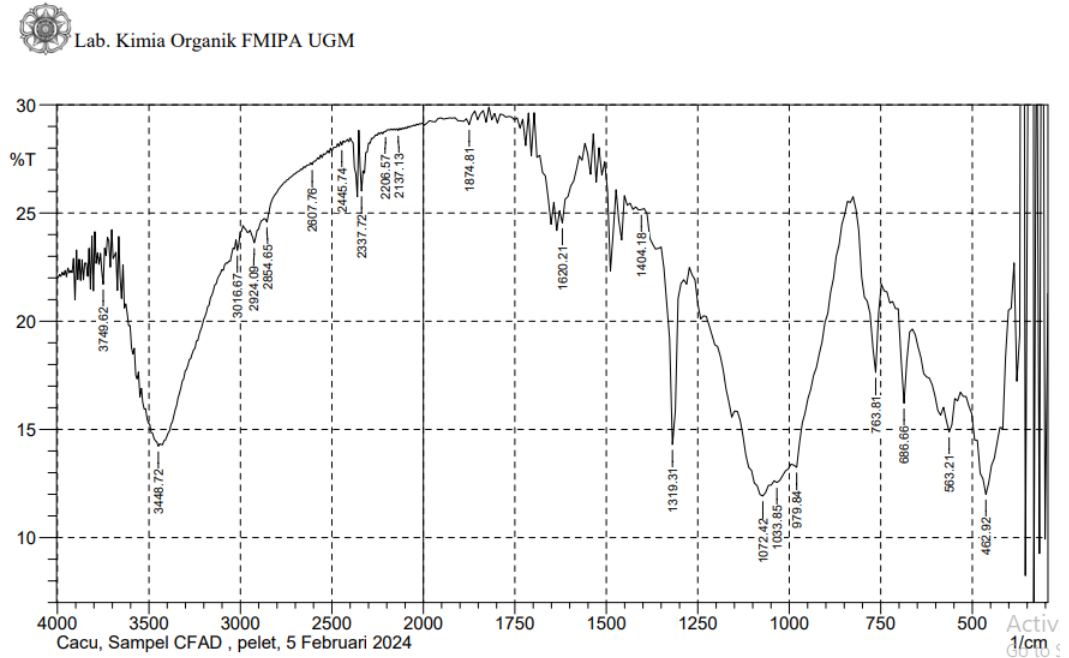
Lampiran 7 Spektra FTIR ALB-Akt-Cd



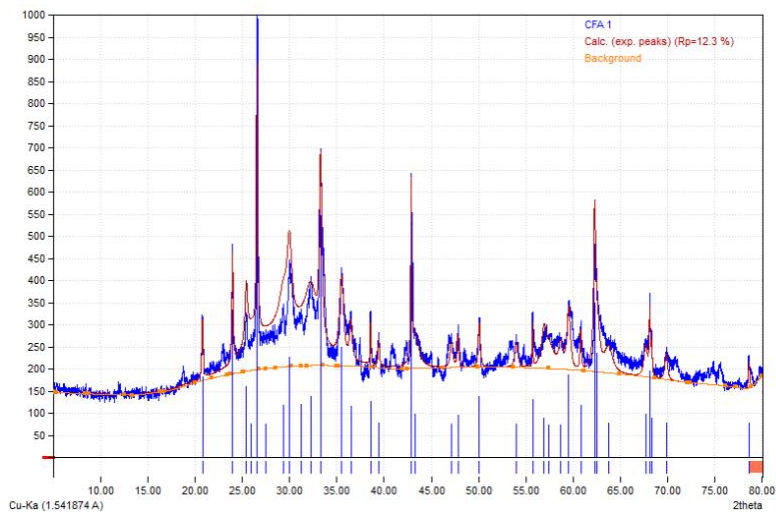
Lampiran 8 Spektra FTIR ALBM-Cd



Lampiran 9 Spektra FTIR ALBM-Dtz-Cd

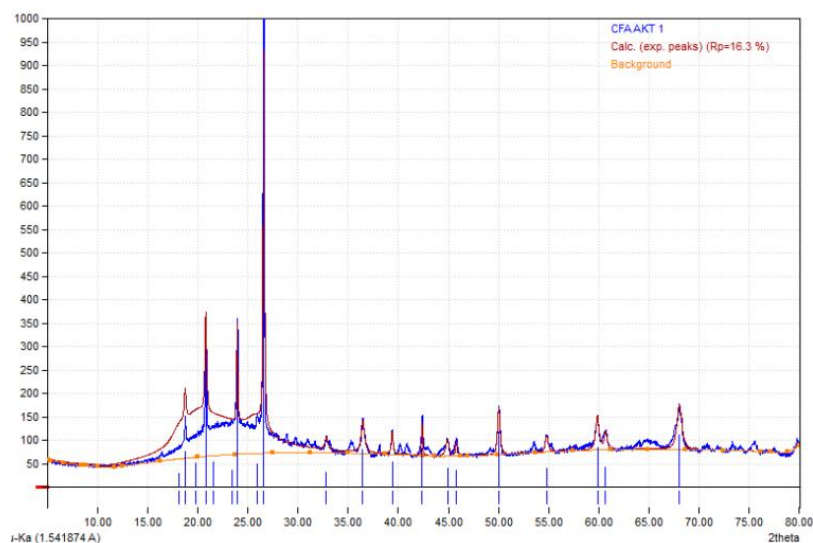


Lampiran 10 Difraktogram ALB



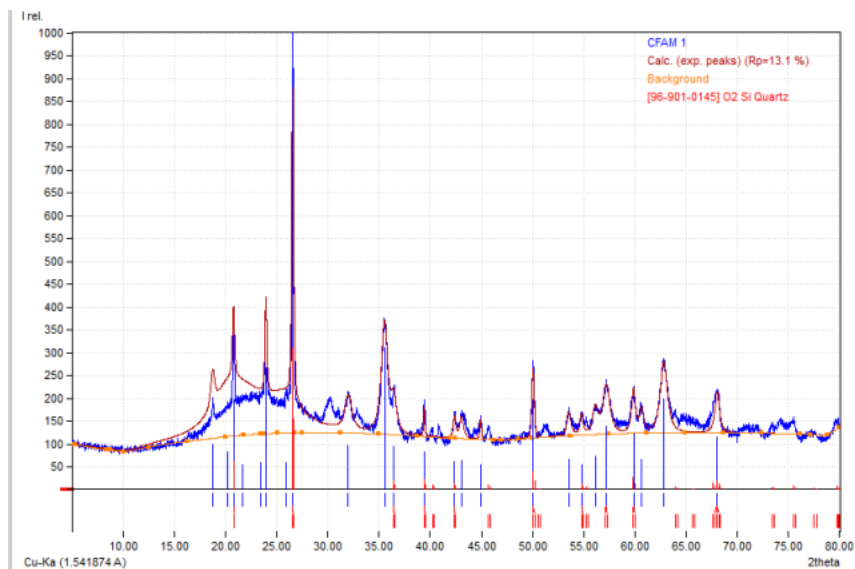
No.	2theta [°]	d [Å]	1/I ₀ (peak height)	Counts (peak area)	FWHM
1	20,80	4,2681	183,52	117,29	0,1637
2	23,99	3,7069	334,59	213,84	0,1637
3	25,44	3,4985	161,30	180,41	0,2864
4	25,91	3,4360	76,57	489,35	1,6368
5	26,59	3,3502	1000,00	639,12	0,1637
6	27,51	3,2401	77,33	1457,91	4,8286
7	29,37	3,0388	118,26	529,06	1,1458
8	30,00	2,9760	228,22	474,04	0,5320
9	31,21	2,8636	120,14	2284,22	4,8695
10	32,27	2,7716	137,93	705,23	1,3094
11	33,30	2,6887	548,34	700,91	0,3274
12	35,51	2,5263	250,71	480,70	0,4910
13	36,49	2,4605	115,62	147,78	0,3274
14	38,57	2,3321	128,31	61,50	0,1228
15	39,43	2,2832	79,41	50,75	0,1637
16	42,89	2,1068	530,82	254,44	0,1228
17	43,28	2,0888	98,19	376,54	0,9821
18	47,13	1,9269	77,47	99,03	0,3274
19	47,82	1,9005	97,54	77,93	0,2046
20	50,07	1,8202	138,64	132,91	0,2455
21	53,98	1,6973	75,93	109,18	0,3683
22	55,72	1,6483	131,68	42,08	0,0818
23	56,91	1,6168	90,25	187,46	0,5320
25	58,69	1,5719	74,26	154,26	0,5320
26	59,53	1,5517	188,09	300,52	0,4092
27	60,79	1,5224	119,88	76,62	0,1637
28	62,27	1,4898	350,35	279,89	0,2046
29	63,74	1,4589	79,61	305,27	0,9821
30	67,67	1,3834	97,82	171,93	0,4501
31	68,12	1,3754	196,07	125,31	0,1637
32	69,84	1,3457	78,46	100,29	0,3274
33	78,59	1,2162	79,40	50,74	0,1637

Lampiran 11 Difraktogram ALB-Akt



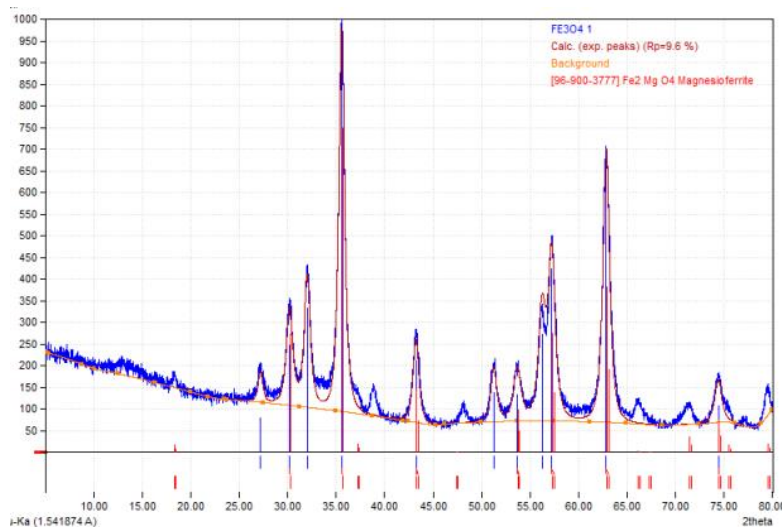
No.	2theta [°]	d [Å]	I/I ₀ (peak height)	Counts (peak area)	FWHM
1	18,16	4,8822	30,10	301,00	1,4731
2	18,77	4,7239	76,39	763,90	0,2046
3	19,81	4,4774	51,42	514,20	2,8235
4	20,82	4,2640	248,66	2486,60	0,2046
5	21,61	4,1083	53,60	5360,00	6,2608
6	23,43	3,7930	36,50	3650,00	9,6162
7	23,97	3,7100	246,69	2466,90	0,1228
8	25,93	3,4333	49,44	494,40	2,3324
9	26,61	3,3477	1000,00	10000,00	0,1637
10	32,83	2,7262	31,35	313,50	0,3274
11	36,47	2,4619	80,89	808,90	0,3683
12	39,39	2,2855	55,25	552,50	0,2046
13	42,38	2,1310	83,18	831,80	0,1228
14	44,90	2,0173	40,96	409,60	0,3683
15	45,78	1,9805	36,40	364,00	0,1637
16	50,03	1,8216	118,47	1184,70	0,2864
17	54,80	1,6738	40,58	405,80	0,3683
18	59,85	1,5440	85,51	855,10	0,4092
19	60,67	1,5251	44,35	443,50	0,3274
20	68,04	1,3769	112,20	1122,00	0,5729

Lampiran 12 Difraktogram ALBM



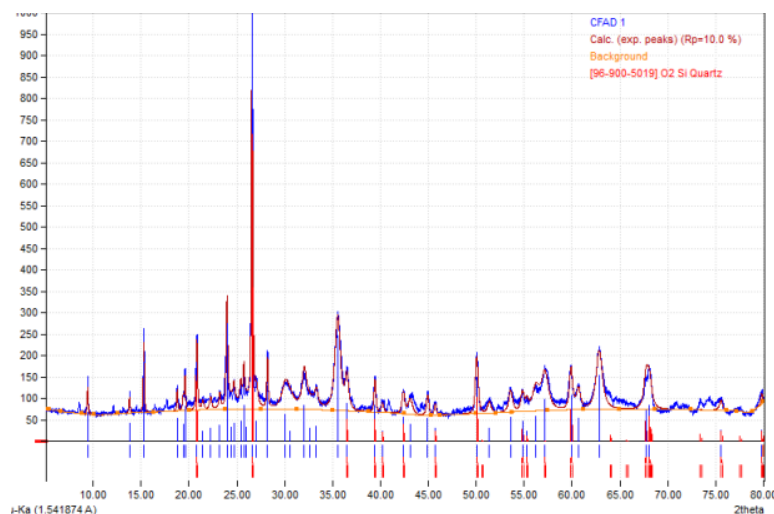
No.	2theta [°]	d [Å]	I/I ₀ (peak height)	Counts (peak area)	FWHM
1	18,77	4,7239	89,90	328,78	0,4501
2	20,22	4,3877	83,15	2060,59	3,3554
3	20,8	4,2681	195,48	354,47	0,2455
4	21,65	4,1007	54,56	1995,17	4,9513
5	23,41	3,7963	58,94	3402,49	7,8157
6	23,97	3,7100	265,57	401,31	0,2046
7	25,95	3,4306	60,11	1344,24	3,0281
8	26,59	3,3502	1000,00	1904,2	0,2046
9	32,01	2,7940	96,32	553,09	0,7775
10	35,55	2,5235	309,99	1686,31	0,7366
11	36,45	2,4632	93,19	422,47	0,6138
12	39,41	2,2843	81,85	74,21	0,1228
13	42,38	2,1310	60,80	128,63	0,2864
14	43,08	2,0982	62,88	190,05	0,4092
15	44,92	2,0164	55,75	67,40	0,1637
16	50,05	1,8209	196,71	356,71	0,2455
17	53,55	1,7099	65,71	218,43	0,4501
18	54,78	1,6744	54,49	148,20	0,3683
19	56,13	1,6373	73,21	331,86	0,6138
20	57,21	1,6088	137,54	831,33	0,8184
21	59,85	1,5440	121,46	403,78	0,4501
22	60,65	1,5256	65,50	237,55	0,491
23	62,82	1,4781	199,00	1202,83	0,8184
24	68,04	1,3769	114,09	448,26	0,5320

Lampiran 13 Difraktogram Fe_3O_4



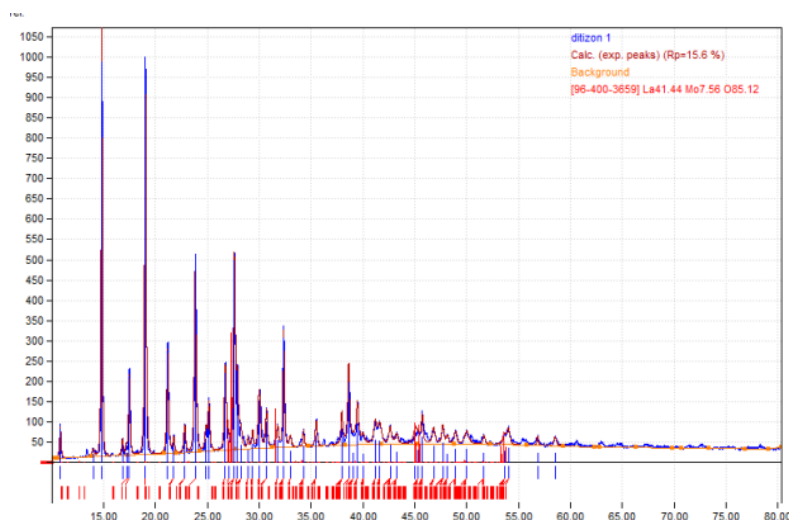
No.	2θ [$^\circ$]	d [Å]	I/I_0 (peak height)	Counts (peak area)	FWHM
1	27,20	3,2760	79,14	79,14	0,5320
2	30,21	2,9563	247,09	247,09	0,7775
3	32,03	2,7923	333,14	333,14	0,7366
4	35,59	2,5207	1000,00	1000	0,6956
5	43,24	2,0907	212,55	212,55	0,6956
6	51,26	1,7808	137,95	137,95	0,6956
7	53,67	1,7063	132,87	132,87	0,9002
8	56,23	1,6346	272,99	272,99	0,9002
9	57,23	1,6083	425,11	425,11	0,8593
10	62,86	1,4772	699,15	699,15	0,8184
11	74,40	1,2741	108,04	108,04	0,8593

Lampiran 14 Difraktogram ALBM-Dtz



No.	2 θ [°]	d [Å]	I/I ₀ (peak height)	Counts (peak area)	FWHM
1	9,45	9,3601	89,67	92,80	0,1228
2	13,81	9,3601	42,02	55,98	0,1228
3	15,30	5,7911	183,82	244,85	0,1228
4	18,80	4,7205	54,84	73,05	0,1228
5	19,60	4,5300	83,18	110,80	0,1228
6	20,82	4,2657	184,08	326,94	0,1637
7	22,26	3,9943	31,92	85,05	0,2455
8	23,22	3,8310	37,93	84,20	0,2046
9	24,00	3,7086	274,65	487,79	0,1637
10	25,43	3,5029	48,66	108,02	0,2046
11	25,76	3,4591	84,19	149,53	0,1637
12	26,00	3,4270	34,61	599,41	0,1637
13	26,61	3,4270	1000,00	1776,07	0,1637
14	27,06	3,1634	47,63	169,18	0,3274
15	28,21	2,9716	130,65	232,05	0,1637
16	30,07	2,9716	63,62	593,22	0,1637
17	32,06	2,7921	85,41	454,57	0,4910
18	35,54	2,5263	248,46	1765,11	0,6547
19	36,50	2,4624	89,53	397,53	0,4092
20	39,42	2,2867	85,78	190,43	0,2046
21	42,39	2,1324	56,35	200,16	0,3274
22	43,13	2,0976	40,86	235,86	0,5320
23	44,93	2,0177	53,50	166,29	0,2864
24	50,06	1,8221	149,96	532,69	0,3274
25	53,60	1,7098	56,24	274,70	0,4501
26	54,83	1,6744	48,28	214,36	0,4092
27	56,24	1,6357	59,15	551,52	0,8593
28	57,18	1,6110	98,98	922,90	0,8593
29	59,90	1,5441	107,97	479,41	0,4092
30	62,85	1,4787	154,05	1299,62	0,7775
31	67,72	1,3837	73,85	393,49	0,4910
32	68,07	1,3775	84,50	562,76	0,6138

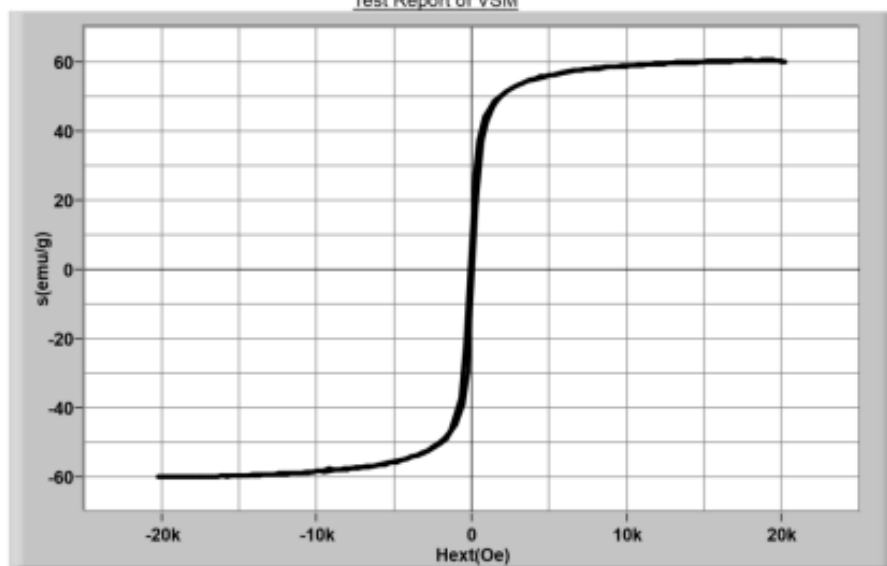
Lampiran 15 Difraktogram ditizon



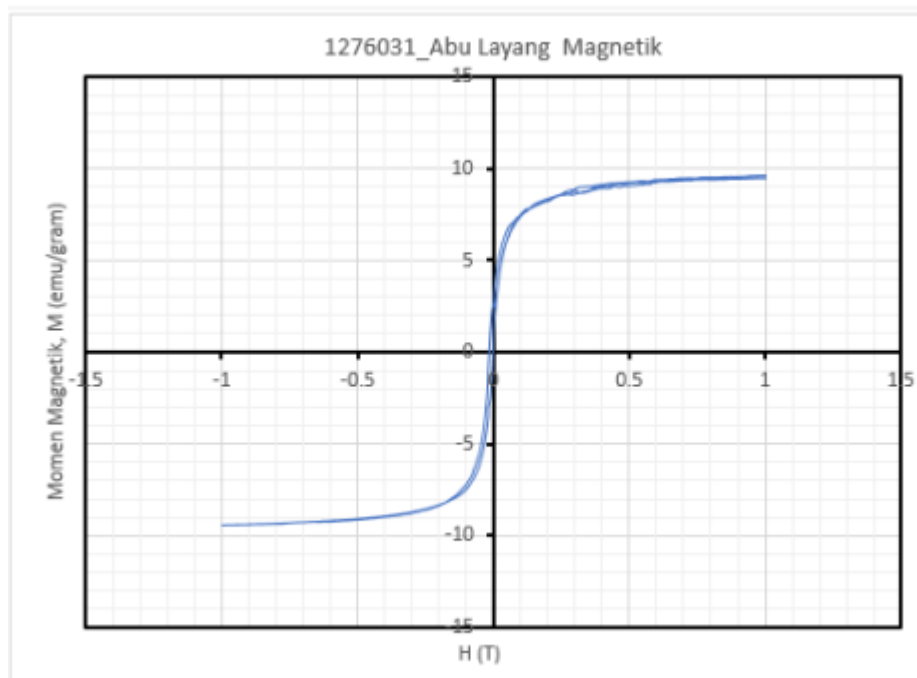
No.	2θ [°]	d [Å]	I/I_0 (peak height)	Counts (peak area)	FWHM
1	10,53	8,3927	363,23	363,23	0,1638
2	14,52	6,0939	986,76	3250,02	0,1228
3	16,53	5,3586	154,24	508,03	0,1228
4	16,90	5,2425	22,54	99,00	0,1638
5	17,18	5,1558	211,21	927,55	0,1638
6	18,74	4,7311	274,27	4391,51	0,1638
7	20,89	4,2489	1505,58	4132,93	0,2047
8	22,53	3,9436	397,18	1234,37	0,2047
9	23,55	3,7745	495,15	2718,04	0,2047
10	24,88	3,5785	125,73	690,19	0,2047
11	26,44	3,3686	220,84	1212,25	0,2047
12	27,32	3,2820	176,27	1161,12	0,2047
13	27,93	3,2288	497,70	2732,08	0,2457
14	30,02	2,9765	152,77	1006,35	0,2456
15	30,72	2,9106	101,27	555,93	0,2047
16	32,38	2,7652	307,27	1349,40	0,1638
17	37,99	2,3688	83,31	457,30	0,2047
18	38,64	2,3302	196,66	1079,54	0,2047
19	39,09	2,3044	23,38	821,50	1,3101
20	41,20	2,1912	56,92	499,89	0,3275
21	41,63	2,1695	52,60	577,49	0,4094
22	42,63	2,1208	43,84	336,91	0,2866
23	45,05	2,0125	26,59	175,14	0,2456
24	45,31	2,0013	30,52	603,12	0,7369
25	45,72	1,9844	64,37	282,67	0,1638
26	46,83	1,9401	41,62	365,51	0,3275
27	47,71	1,9063	47,50	312,92	0,2456
28	48,92	1,8620	33,22	255,27	0,2866
29	50,02	1,8234	34,37	415,05	0,4503
30	53,71	1,7067	28,51	344,25	0,4503
31	54,05	1,6966	37,19	244,97	0,2456
32	56,86	1,6194	23,09	101,40	0,1638
32	58,54	1,5769	23,45	180,23	0,2866

Lampiran 16 Data magnetisasi menggunakan VSM

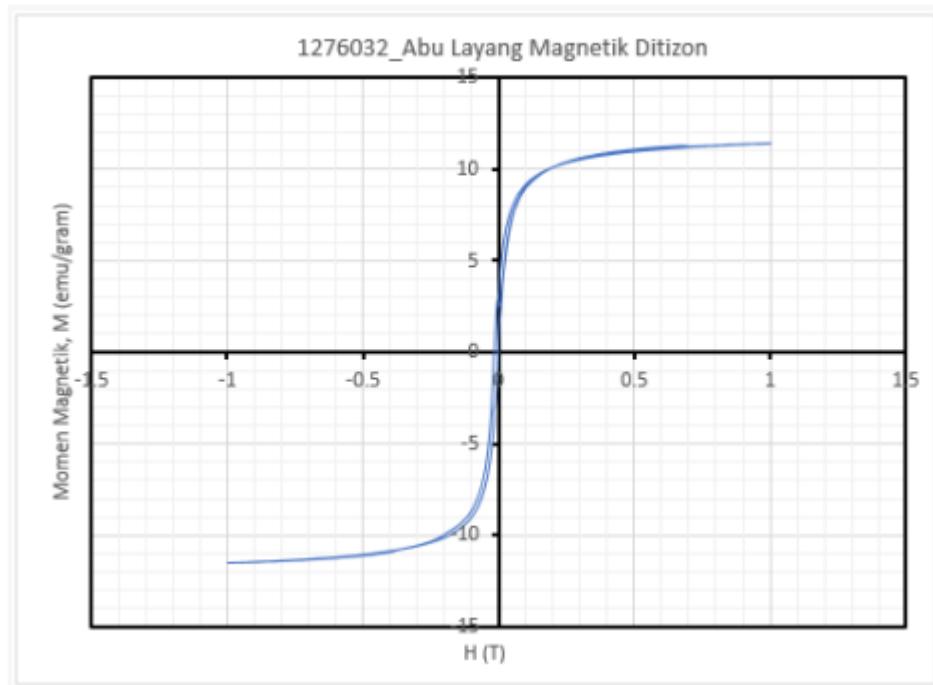
- Kurva histeresis Fe_3O_4



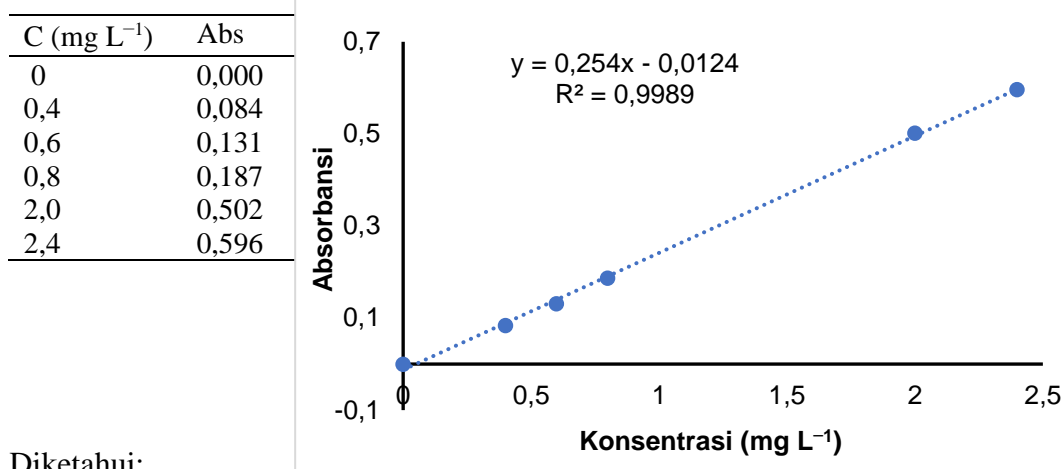
- Kurva histeresis ALBM



- Kurva histeresis ALBM-Dtz



Lampiran 17 Data pengaruh pH terhadap adsorpsi Cd(II)



Diketahui:

Massa adsorben : 20 mg

Konsentrasi awal ion Cd(II) : 20 mg L⁻¹

Volume adsorbat : 20 mL

Waktu kontak adsorpsi : 60 menit

Tabel pengaruh pH terhadap adsorpsi Cd(II) pada adsorben ALB-Akt

	A ₀	C ₀ (mg L ⁻¹)	A _e	C _e (mg L ⁻¹)	C ₀ -C _e (mg L ⁻¹)	C ₀ -C _e (V) (mg L ⁻¹)	q _e (mg g ⁻¹)
3	0,246	20,346	0,182	15,307	5,039	0,101	5,039
4	0,270	22,236	0,151	12,866	9,370	0,187	9,370
5	0,256	21,134	0,128	11,055	10,079	0,202	10,079
6	0,258	21,291	0,102	9,008	12,283	0,246	12,283
7	0,242	20,031	0,113	9,874	10,157	0,203	10,157
8	0,201	16,803	0,135	11,606	5,197	0,104	5,197

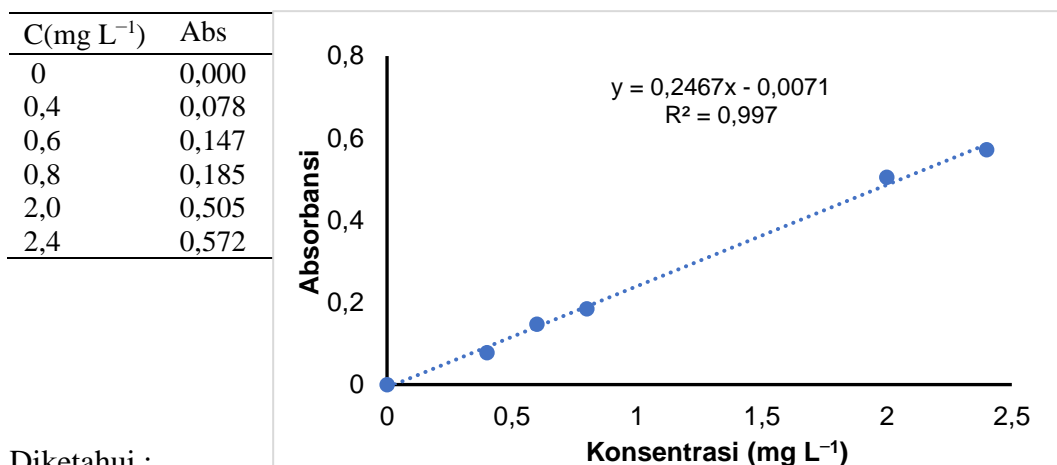
Tabel pengaruh pH terhadap adsorpsi ion Cd(II) pada adsorben ALBM

pH	A ₀	C ₀ (mg L ⁻¹)	A _e	C _e (mg L ⁻¹)	C ₀ -C _e (mg L ⁻¹)	C ₀ -C _e (V) (mg L ⁻¹)	q _e (mg g ⁻¹)
3	0,246	20,346	0,146	12,472	7,874	0,157	7,874
4	0,270	22,236	0,117	10,189	12,047	0,241	12,047
5	0,256	21,134	0,091	8,142	12,992	0,260	12,992
6	0,258	21,291	0,089	7,984	13,307	0,266	13,307
7	0,242	20,031	0,082	7,433	12,598	0,252	12,598
8	0,201	16,803	0,069	6,409	10,394	0,208	10,394

Tabel pengaruh pH terhadap adsorpsi ion Cd(II) pada adsorben ALBM-Dtz

pH	A_0	C_0 (mg L ⁻¹)	A_e	C_e (mg L ⁻¹)	$C_0 - C_e$ (mg L ⁻¹)	$C_0 - C_e(V)$ (mg L ⁻¹)	q_e (mg g ⁻¹)
3	0,246	20,346	0,127	10,976	9,370	0,187	9,370
4	0,270	22,236	0,128	11,055	11,181	0,224	11,181
5	0,256	21,134	0,077	7,039	14,094	0,282	14,094
6	0,258	21,291	0,049	4,835	16,457	0,329	16,457
7	0,242	20,031	0,058	5,543	14,488	0,290	14,488
8	0,201	16,803	0,080	7,276	9,528	0,191	9,528

Lampiran 18 Data pengaruh massa terhadap adsorpsi Cd(II)



Diketahui :

Konsentrasi awal ion Cd(II) : 20 mg L⁻¹

Volume adsorbat : 20 mL

pH : 6

Waktu : 60 menit

Tabel pengaruh massa terhadap adsorpsi ion Cd(II) pada adsorben ALB-Akt

Massa Adsorben (mg)	A ₀	C ₀ (mg L ⁻¹)	A _e	C _e (mg L ⁻¹)	C ₀ -C _e (mg L ⁻¹)	C ₀ -C _e (V) (mg L ⁻¹)	q _e (mg g ⁻¹)
5	0,251	20,527	0,095	8,067	12,460	0,249	49,840
10	0,251	20,527	0,067	5,831	14,696	0,294	29,393
20	0,251	20,527	0,066	5,751	14,776	0,296	14,776
30	0,251	20,527	0,065	5,671	14,856	0,297	9,904
40	0,251	20,527	0,040	3,674	16,853	0,337	10,157
60	0,251	20,527	0,056	4,952	15,575	0,312	8,427
100	0,251	20,527	0,068	5,911	14,617	0,292	2,923

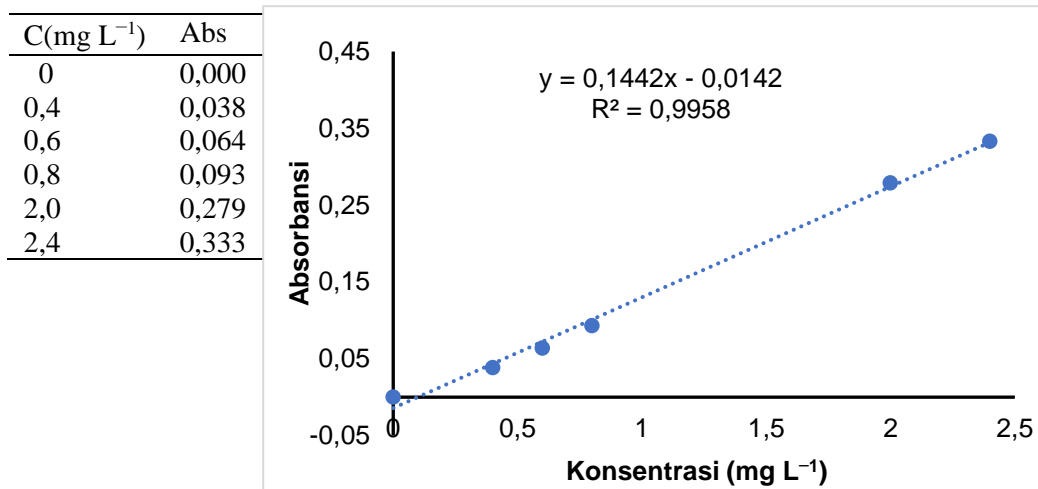
Tabel pengaruh massa terhadap adsorpsi ion Cd(II) pada adsorben ALBM

Massa Adsorben (mg)	A ₀	C ₀ (mg L ⁻¹)	A _e	C _e (mg L ⁻¹)	C ₀ -C _e (mg L ⁻¹)	C ₀ -C _e (V) (mg L ⁻¹)	q _e (mg g ⁻¹)
5	0,251	20,527	0,143	11,901	8,626	0,173	34,505
10	0,251	20,527	0,096	8,147	12,380	0,248	24,760
20	0,251	20,527	0,088	7,508	13,019	0,260	13,019
30	0,251	20,527	0,076	6,550	13,978	0,280	9,318
40	0,251	20,527	0,059	5,192	15,335	0,307	7,668
60	0,251	20,527	0,059	5,192	15,335	0,307	5,112
100	0,251	20,527	0,060	5,272	15,256	0,305	3,051

Tabel pengaruh massa terhadap adsorpsi ion Cd(II) pada adsorben ALBM-Dtz

Massa Adsorben (mg)	A_0	C_0 (mg L ⁻¹)	A_e	C_e (mg L ⁻¹)	$C_0 - C_e$ (mg L ⁻¹)	$C_0 - C_e(V)$ (mg L ⁻¹)	q_e (mg g ⁻¹)
5	0,251	20,527	0,077	6,629	13,898	0,278	55,591
10	0,251	20,527	0,066	5,751	14,776	0,296	29,553
20	0,251	20,527	0,045	4,073	16,454	0,329	16,454
30	0,251	20,527	0,039	3,594	16,933	0,339	11,289
40	0,251	20,527	0,028	2,716	17,812	0,356	8,906
60	0,251	20,527	0,035	3,275	17,252	0,345	5,751
100	0,251	20,527	0,060	3,435	17,093	0,342	3,419

Lampiran 19 Data pengaruh waktu terhadap adsorpsi Cd(II)



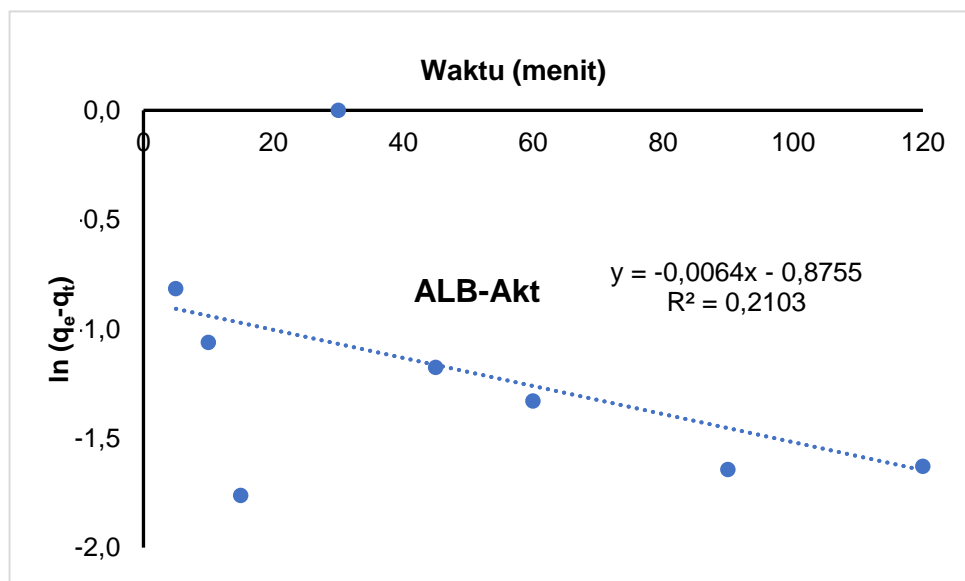
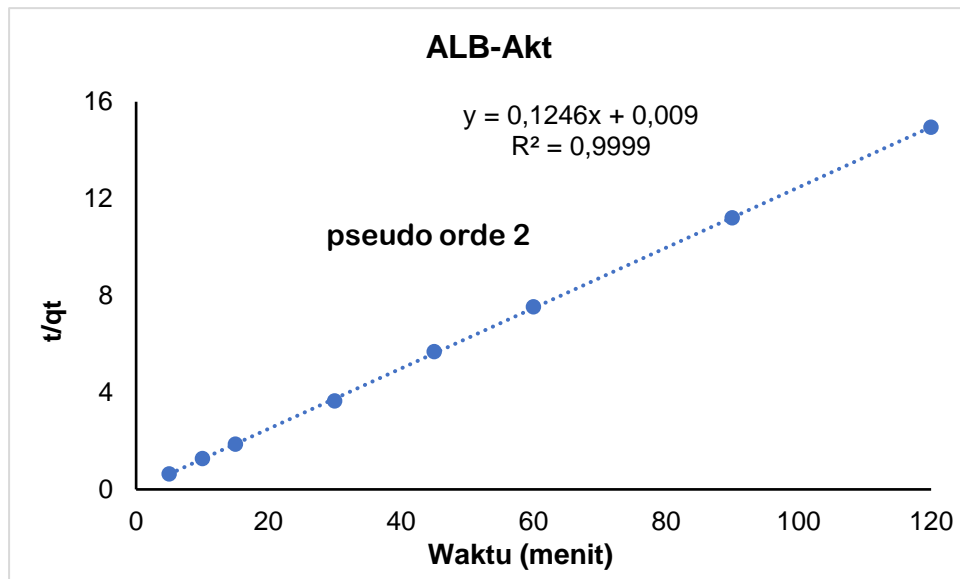
Diketahui:

pH : 6
 Massa adsorben : 40 mg
 Konsentrasi awal ion Cd(II) : 20 mg L⁻¹
 Volume adsorbat : 20 mL

Tabel pengaruh waktu terhadap adsorpsi ion Cd(II) pada adsorben ALB-Akt

Waktu (menit)	A ₀	A _e	C ₀ (mg L ⁻¹)	C _e (mg L ⁻¹)
5	0,136	0,023	20,793	5,227
10	0,136	0,022	20,793	5,035
15	0,136	0,020	20,793	4,687
30	0,136	0,017	20,793	4,343
45	0,136	0,022	20,793	4,960
60	0,136	0,021	20,793	4,872
90	0,136	0,020	20,793	4,730
120	0,136	0,020	20,793	4,735

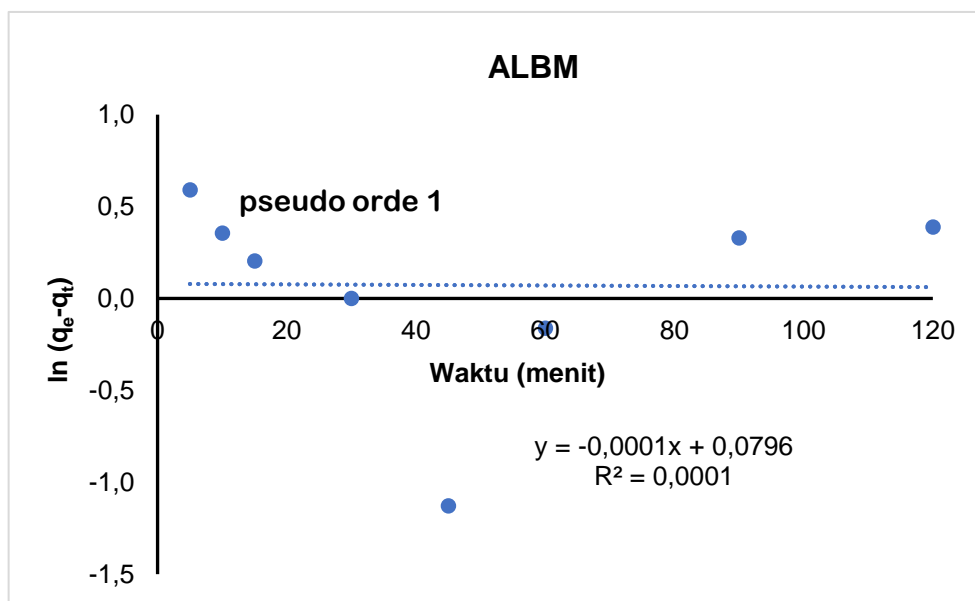
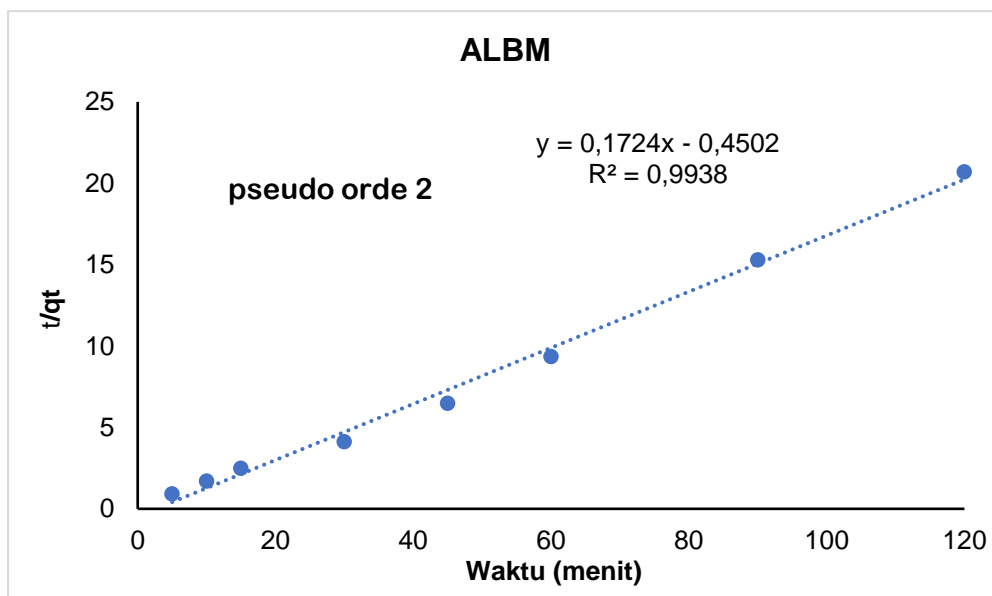
C ₀ -C _e (mg L ⁻¹)	C ₀ -C _e (V) (mg L ⁻¹)	q _e (mg g ⁻¹)	q _t (mg g ⁻¹)	t/q _t	ln (q _e -q _t)
15,566	0,311	8,225	7,783	0,642	-0,815
15,759	0,315	8,225	7,879	1,269	-1,061
16,107	0,322	8,225	8,053	1,863	-1,760
16,451	0,329	8,225	8,225	3,647	#NUM!
15,834	0,317	8,225	7,917	5,684	-1,176
15,921	0,318	8,225	7,960	7,537	-1,328
16,064	0,321	8,225	8,032	11,205	-1,643
16,058	0,321	8,225	8,029	14,946	-1,628



Tabel pengaruh waktu terhadap adsorpsi ion Cd(II) pada adsorben ALBM

Waktu (menit)	A_0	A_e	C_0 (mg L ⁻¹)	C_e (mg L ⁻¹)
5	0,136	0,057	20,793	9,861
10	0,136	0,051	20,793	9,104
15	0,136	0,049	20,793	8,700
30	0,136	0,031	20,793	6,248
45	0,136	0,036	20,793	6,896
60	0,136	0,043	20,793	7,950
90	0,136	0,051	20,793	9,029
120	0,136	0,052	20,793	9,198

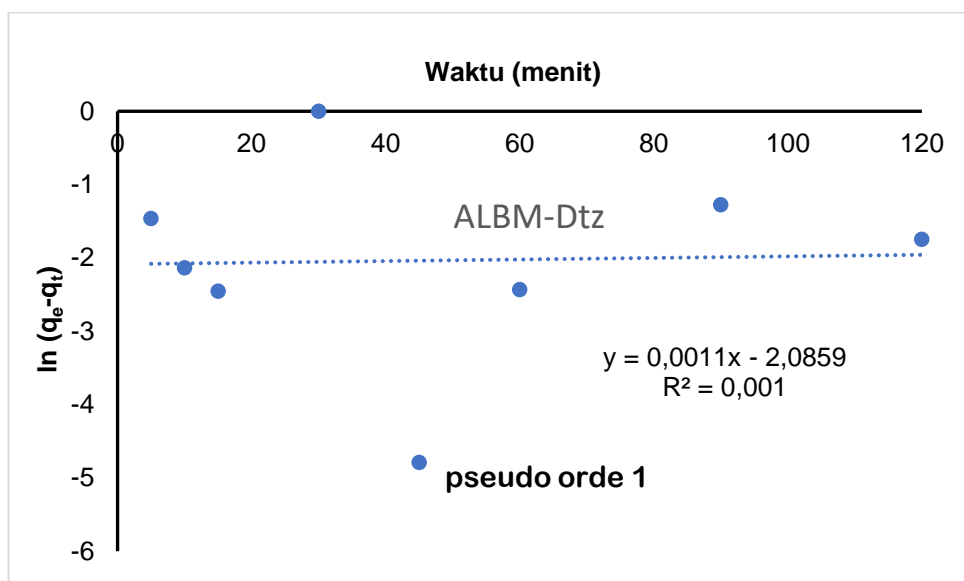
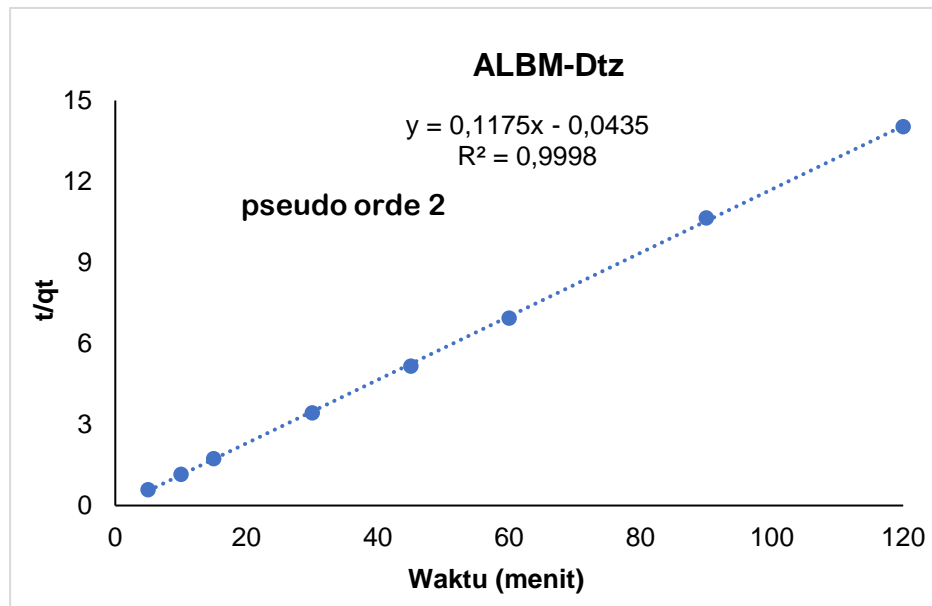
C_0-C_e (mg L ⁻¹)	$C_0-C_e(V)$ (mg L ⁻¹)	q_e (mg g ⁻¹)	q_t (mg g ⁻¹)	t/q_t	$\ln (q_e-q_t)$
10,932	0,219	7,273	5,466	0,915	0,591
11,689	0,234	7,273	5,845	1,711	0,356
12,093	0,242	7,273	6,046	2,481	0,204
14,545	0,291	7,273	7,273	4,125	#NUM!
13,897	0,278	7,273	6,949	6,476	-1,127
12,843	0,257	7,273	6,422	9,343	-0,161
11,764	0,235	7,273	5,882	15,301	0,330
11,595	0,232	7,273	5,798	20,699	0,389



Tabel pengaruh waktu terhadap adsorpsi ion Cd(II) pada adsorben ALBM-Dtz

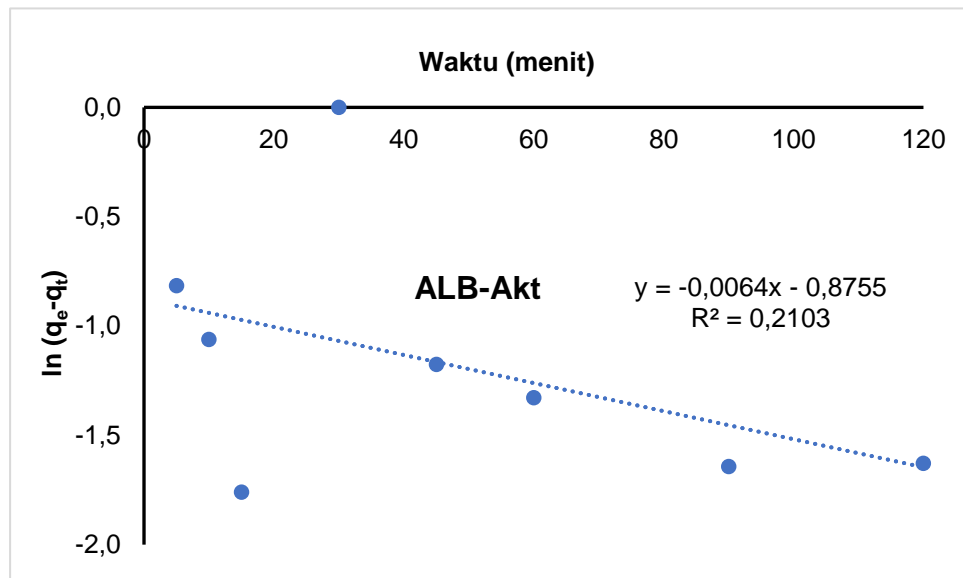
Waktu (menit)	A_0	A_e	C_0 (mg L ⁻¹)	C_e (mg L ⁻¹)
5	0,136	0,013	20,793	3,809
10	0,136	0,012	20,793	3,583
15	0,136	0,011	20,793	3,517
30	0,136	0,010	20,793	3,345
45	0,136	0,010	20,793	3,362
60	0,136	0,011	20,793	3,521
90	0,136	0,014	20,793	3,904
120	0,136	0,012	20,793	3,695

C_0-C_e (mg L ⁻¹)	$C_0-C_e(V)$ (mg L ⁻¹)	q_e (mg g ⁻¹)	q_t (mg g ⁻¹)	t/q_t	$\ln (q_e-q_t)$
16,985	0,340	8,724	8,492	0,589	-1,463
17,211	0,344	8,724	8,605	1,162	-2,132
17,276	0,346	8,724	8,638	1,737	-2,454
17,448	0,349	8,724	8,724	3,439	#NUM!
17,431	0,349	8,724	8,716	5,163	-4,789
17,272	0,345	8,724	8,636	6,948	-2,430
16,889	0,338	8,724	8,445	10,658	-1,275
17,098	0,342	8,724	8,549	14,036	-1,744



Lampiran 20 Persamaan kinetika adsorpsi

Persamaan kinetika orde kesatu semu untuk adsorpsi Cd(II) pada adsorben ALB-Akt



$$\ln q_e - q_t = \ln q_e - \beta t$$

Jika diambil plot $\ln q_e - q_t$ lawan t , akan diperoleh garis lurus dengan β sebagai *slope*, sehingga:

Persamaan garis lurus

$$Y = -0,0064x - 0,8755$$

$$R^2 = 0,2103$$

Maka

$$\text{Slope} = -\beta t$$

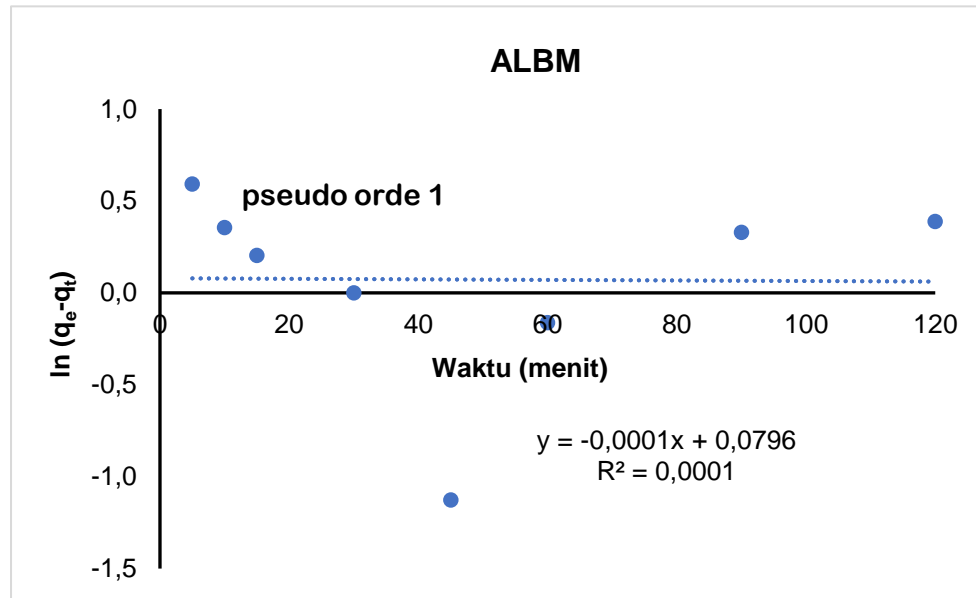
$$\beta = 0,0064 \text{ menit}^{-1}$$

$$\text{intersep } \ln q_e = -0,8755$$

$$e^{-0,8755} = 9,80 \times 10^{-1} \text{ mol g}^{-1}$$

$$q_e = 9,80 \times 10^{-1} \text{ mol g}^{-1}$$

Persamaan kinetika orde kesatu semu untuk adsorpsi Cd(II) pada adsorben ALBM



$$\ln q_e - q_t = \ln q_e - \beta t$$

Jika diambil plot $\ln q_e - q_t$ lawan t , akan diperoleh garis lurus dengan β sebagai *slope*, sehingga:

Persamaan garis lurus

$$Y = 0,0001x - 0,5204$$

$$R^2 = 0,0102$$

Maka

$$\text{Slope} = -\beta t$$

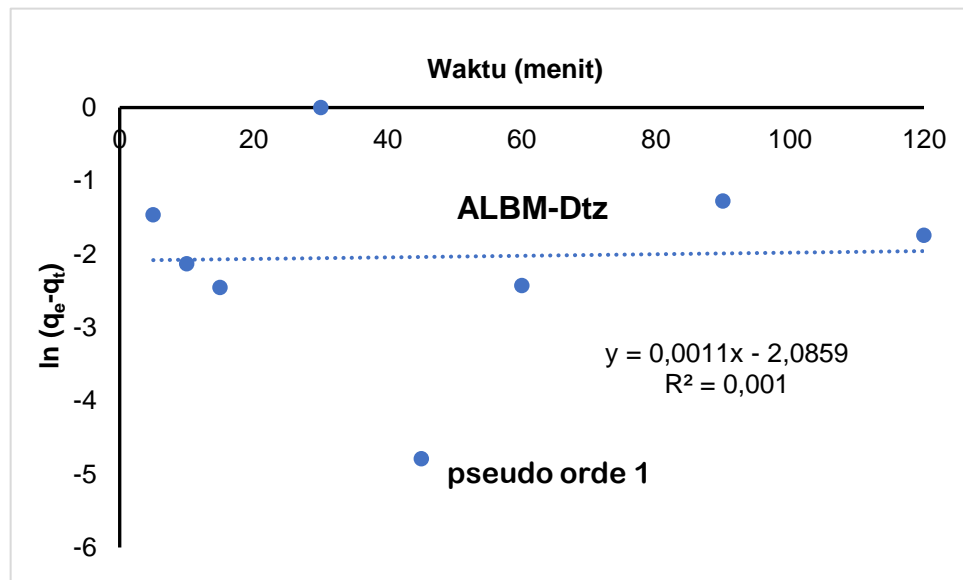
$$B = -0,0001 \text{ menit}^{-1}$$

$$\text{intersep } \ln q_e = -0,5204$$

$$e^{-0,5204} = 9,99 \times 10^{-1} \text{ mol g}^{-1}$$

$$q_e = 9,99 \times 10^{-1} \text{ mol g}^{-1}$$

Persamaan kinetika orde kesatu semu untuk adsorpsi Cd(II) pada adsorben ALBM-Dtz



$$\ln q_e - q_t = \ln q_e - \beta t$$

Jika diambil plot $\ln q_e - q_t$ lawan t , akan diperoleh garis lurus dengan β sebagai *slope*, sehingga:

Persamaan garis lurus

$$Y = 0,0011x - 2,0859$$

$$R^2 = 0,001$$

Maka

$$\text{Slope} = -\beta$$

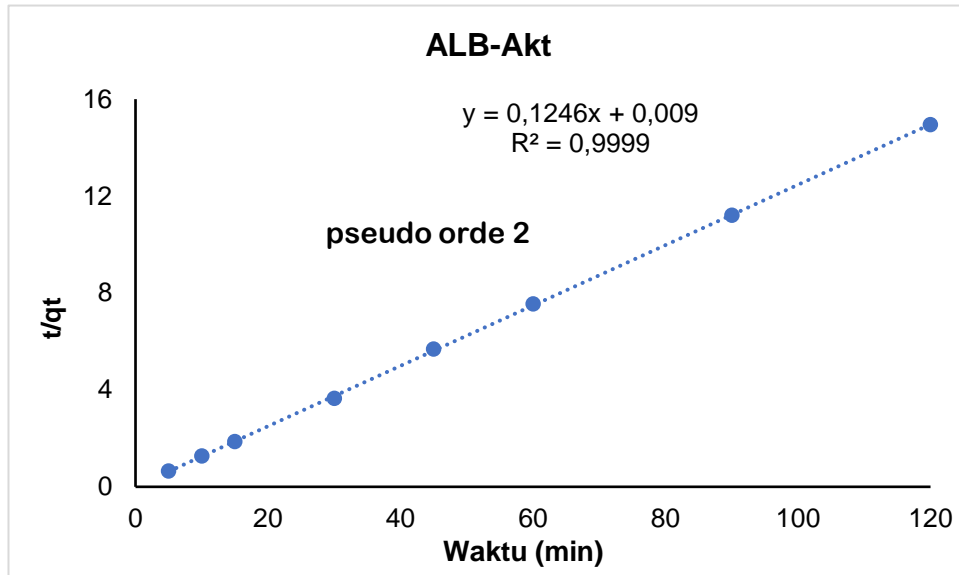
$$\beta = -0,0011 \text{ menit}^{-1}$$

$$\text{intersep } \ln q_e = -2,0859$$

$$e^{-2,0859} = 1,002 \text{ mol g}^{-1}$$

$$q_e = 1,002 \text{ mol g}^{-1}$$

Persamaan kinetika orde kedua semu untuk adsorpsi Cd(II) pada adsorben ALB-Akt



$$t/q_t = 1/(k_2 \cdot q_e^2) + 1/q_e \cdot t$$

Jika diambil plot t/q_t lawan t , maka akan diperoleh garis lurus dengan nilai $1/q_e$ sebagai *slope* dan $1/k_2 \cdot q_e^2$ sebagai intersep, sehingga:

Persamaan garis lurus

$$Y = 0,1246x + 0,009$$

$$R^2 = 0,9999$$

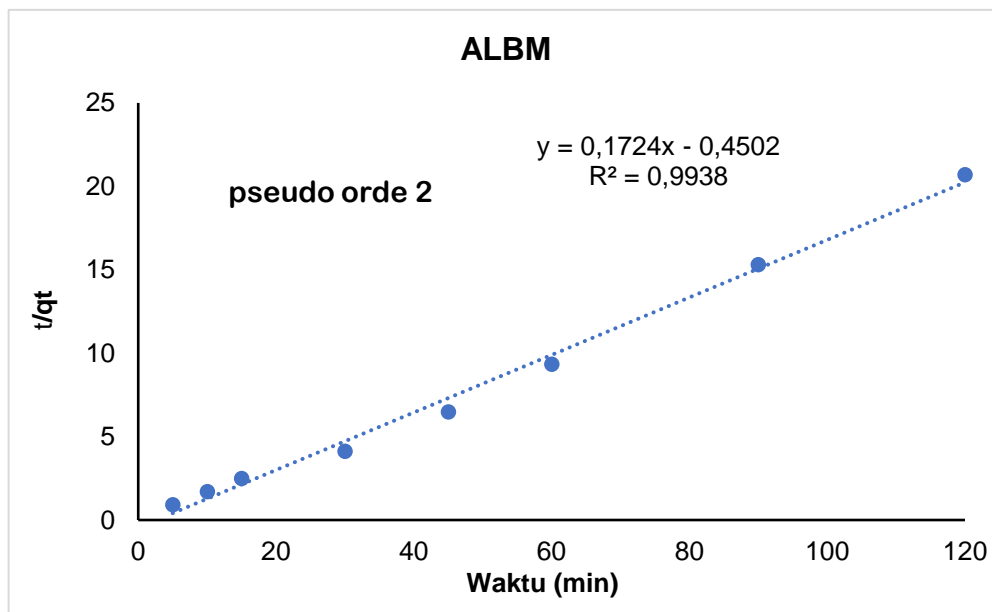
Maka

$$1/q_e = 0,1246 \rightarrow q_e = 8,026 \text{ mg g}^{-1}$$

$$1/(k_2 \cdot q_e^2) = 0,009 \rightarrow 1/(k_2 \cdot (8,026)^2) = 0,009$$

$$k_2 = 1,725 \text{ g mg}^{-1} \text{ menit}^{-1}$$

Persamaan kinetika orde kedua semu untuk adsorpsi Cd(II) pada adsorben ALBM



$$t/q_t = 1/(k_2 \cdot q_e^2) + 1/q_e \cdot t$$

Jika diambil plot t/q_t lawan t , maka akan diperoleh garis lurus dengan nilai $1/q_e$ sebagai *slope* dan $1/k_2 \cdot q_e^2$ sebagai intersep, sehingga :

Persamaan garis lurus

$$Y = 0,1724x - 0,4502$$

$$R^2 = 0,9938$$

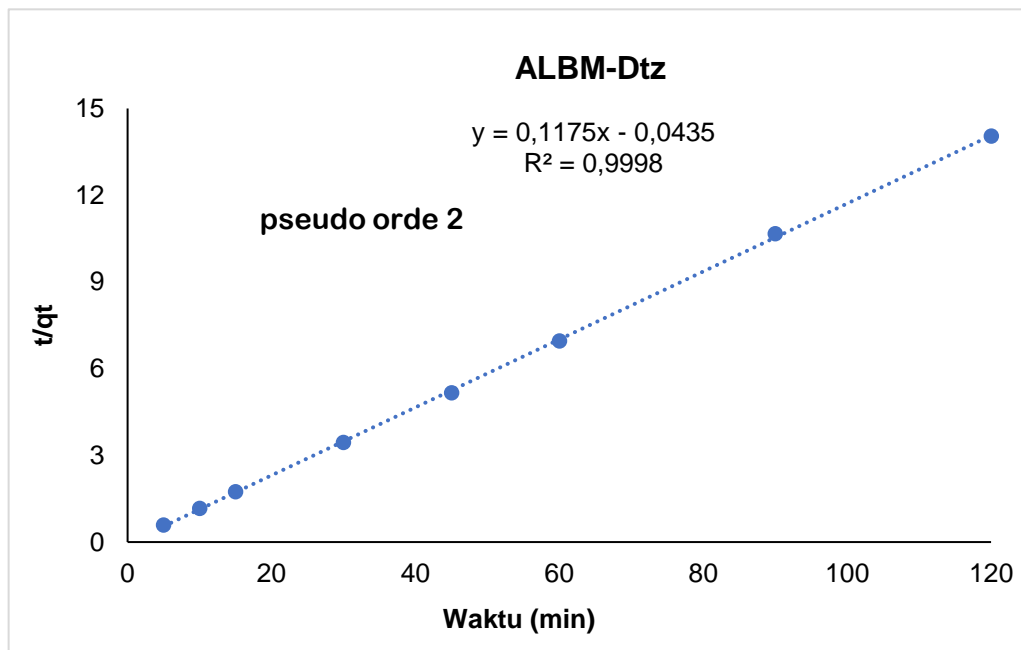
Maka

$$1/q_e = 0,1724 \rightarrow q_e = 5,8 \text{ mg g}^{-1}$$

$$1/(k_2 \cdot q_e^2) = -0,4502 \rightarrow 1/(k_2 \cdot (5,8)^2) = -0,4502$$

$$k_2 = -0,066 \text{ g mg}^{-1} \text{ menit}^{-1}$$

Persamaan kinetika orde kedua semu untuk adsorpsi Cd(II) pada adsorben ALBM-Dtz



$$t/q_t = 1/(k_2 \cdot q_e^2) + 1/q_e \cdot t$$

Jika diambil plot t/q_t lawan t , maka akan diperoleh garis lurus dengan nilai $1/q_e$ sebagai *slope* dan $1/k_2 \cdot q_e^2$ sebagai intersep, sehingga :

Persamaan garis lurus

$$Y = 0,1175x - 0,0435$$

$$R^2 = 0,9998$$

Maka

$$1/q_e = 0,1175 \rightarrow q_e = 8,51 \text{ mg g}^{-1}$$

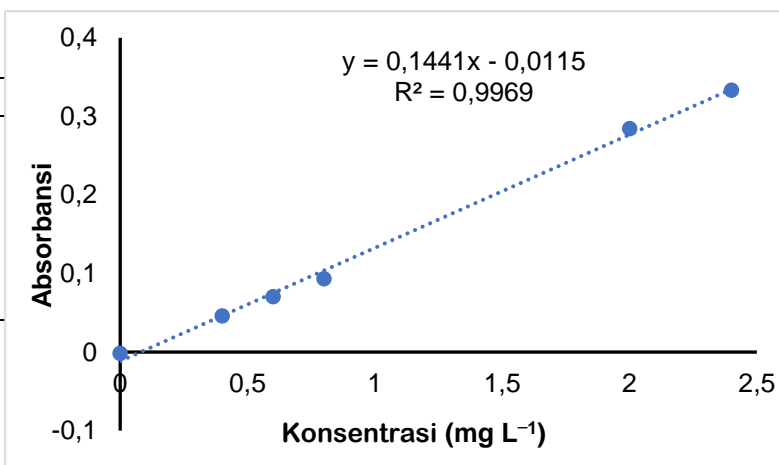
$$1/(k_2 \cdot q_e^2) = -0,0435 \rightarrow 1/(k_2 \cdot (8,51)^2) = -0,0435$$

$$k_2 = -0,317 \text{ g mg}^{-1} \text{ menit}^{-1}$$

Lampiran 21 Data pengaruh konsentrasi terhadap adsorpsi Cd(II)

Larutan Standar Cd(II)

C(mg L ⁻¹)	Abs
0	-0,001
0,4	0,045
0,6	0,070
0,8	0,093
2,0	0,284
2,4	0,333



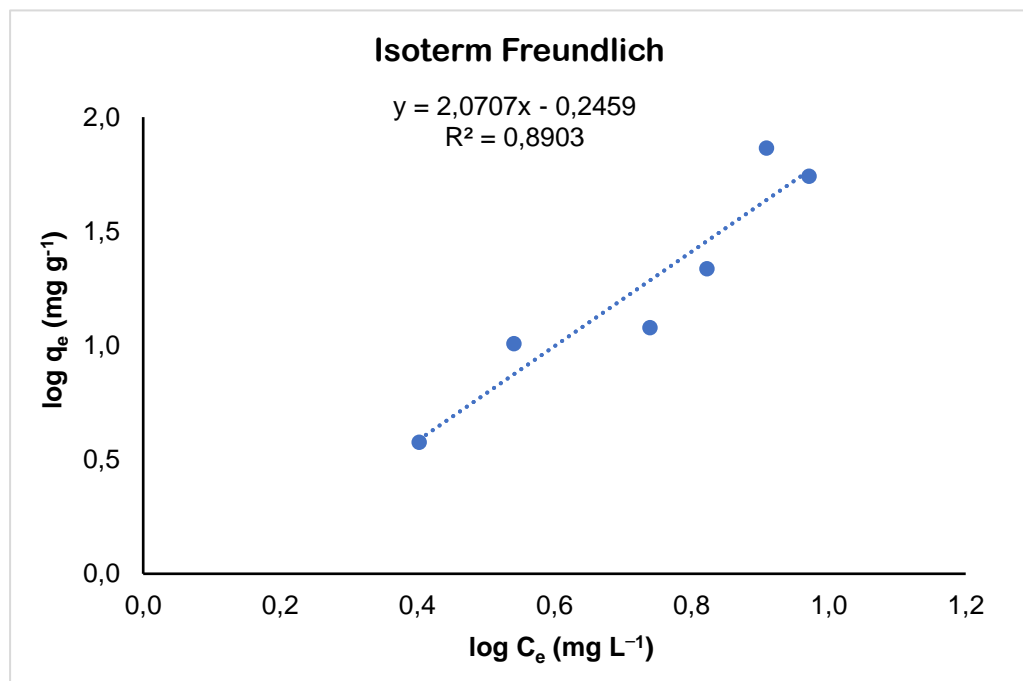
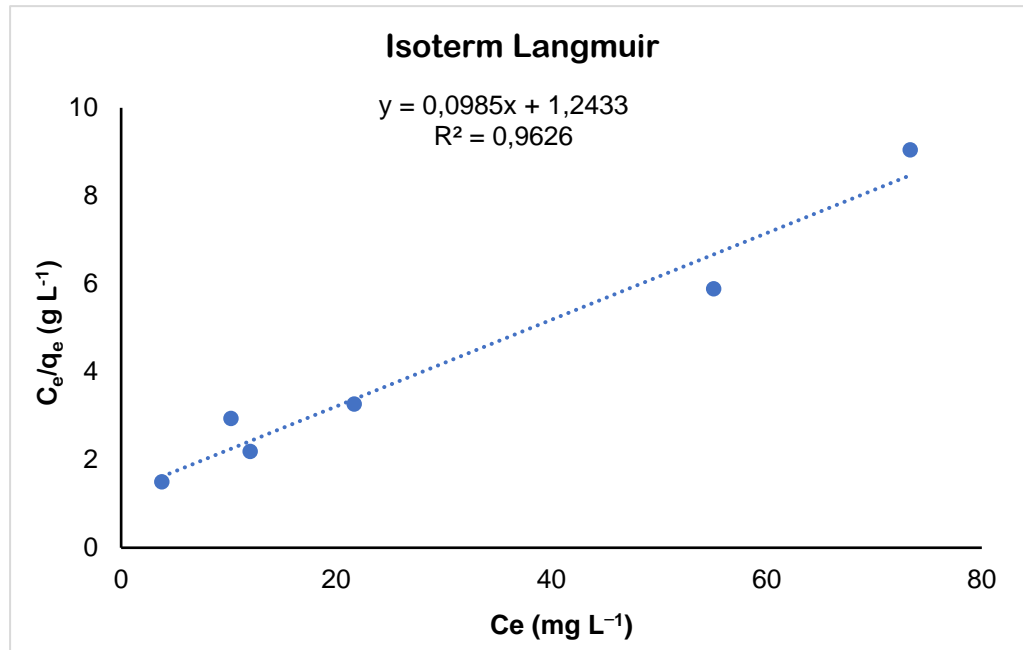
Diketahui :

pH : 6
 Massa adsorben : 40 mg
 Volume adsorbat : 20 mL
 Waktu kontak adsorpsi : 30 menit

Tabel pengaruh konsentrasi terhadap adsorpsi ion Cd(II) pada adsorben ALB-Akt

Konsentrasi	A ₀	A _e	fp	C ₀ (mg L ⁻¹)	C _e (mg L ⁻¹)
10	0,116	0,043	10	8,827	3,775
20	0,236	0,135	10	17,146	10,194
30	0,209	0,104	15	22,974	12,000
40	0,240	0,145	20	34,963	21,674
60	0,254	0,187	40	73,810	55,081
80	0,311	0,253	40	89,566	73,338

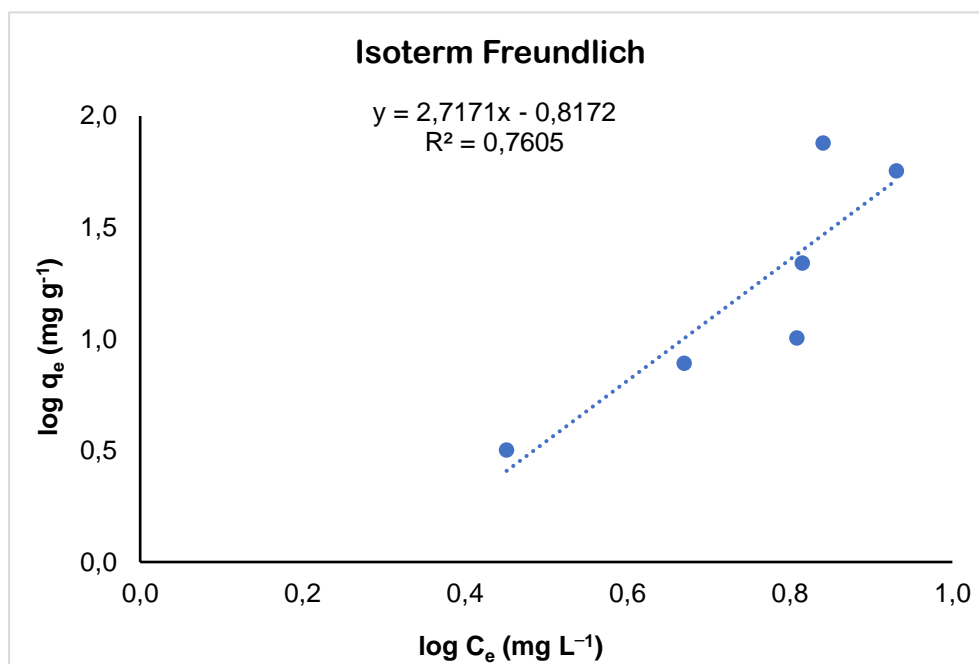
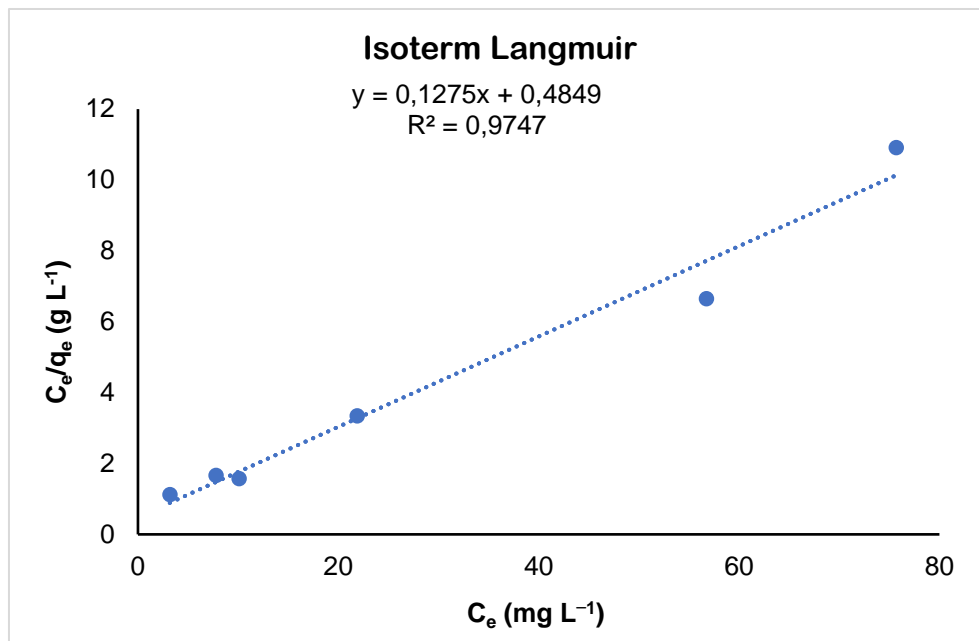
C ₀ -C _e (mg L ⁻¹)	q _e (mg g ⁻¹)	c _e /q _e	log q _e	log c _e	ln c _e
5,052	2,526	1,495	0,402	0,577	1,328
6,592	3,476	2,933	0,541	1,008	2,322
10,974	5,487	2,187	0,739	1,079	2,485
13,289	6,645	3,262	0,822	1,336	3,076
18,729	9,364	5,882	0,971	1,741	4,009
16,228	8,114	9,039	0,909	1,865	4,295



Tabel pengaruh konsentrasi terhadap adsorpsi ion Cd(II) pada adsorben ALBM

Konsentrasi	A_0	A_e	f_p	C_0 (mg L ⁻¹)	C_e (mg L ⁻¹)
10	0,116	0,034	10	8,827	3,176
20	0,236	0,101	10	17,146	7,793
30	0,209	0,086	15	22,974	10,102
40	0,240	0,146	20	34,963	21,883
60	0,254	0,193	40	73,810	56,741
80	0,311	0,261	40	89,566	75,695

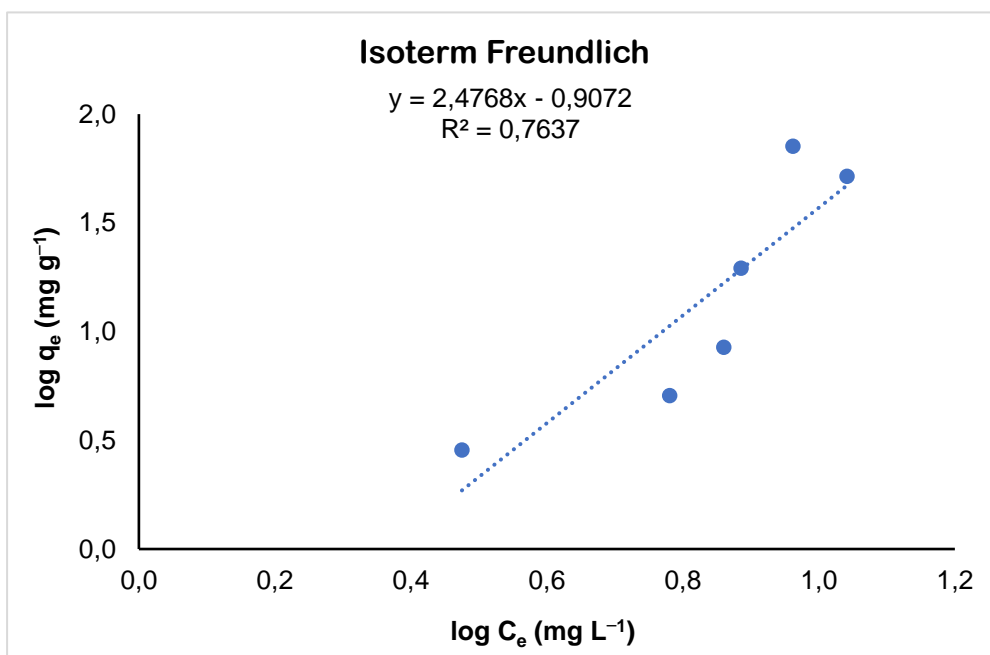
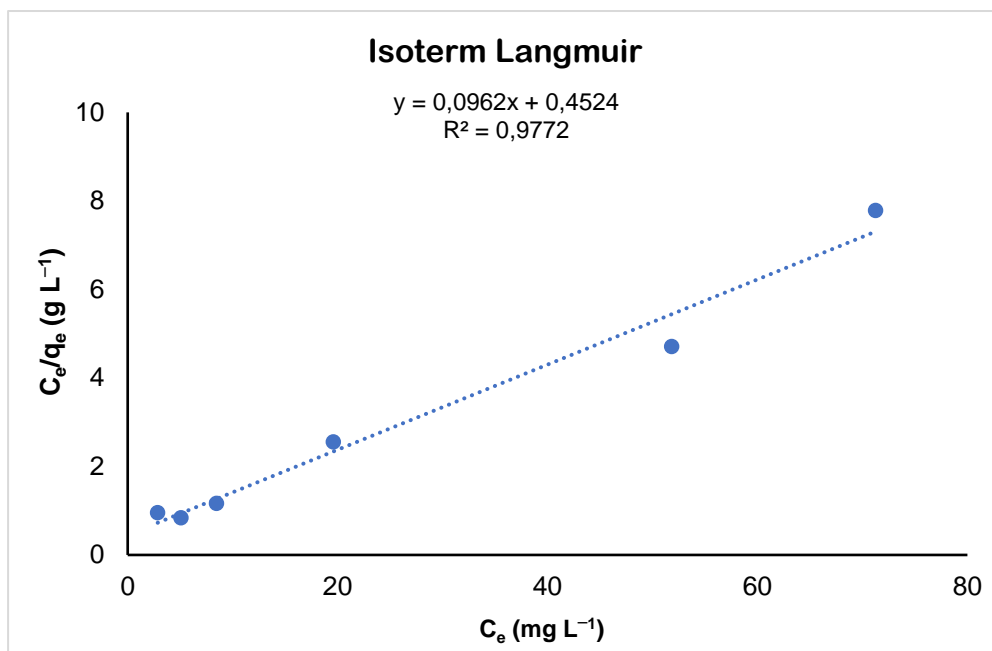
$C_0 - C_e$ (mg L ⁻¹)	q_e (mg g ⁻¹)	c_e/q_e	$\log q_e$	$\log c_e$	$\ln c_e$
5,651	2,825	1,124	0,451	0,502	1,156
9,353	4,677	1,666	0,670	0,892	2,053
12,871	6,436	1,570	0,809	1,004	2,313
13,080	6,540	3,346	0,816	1,340	3,086
17,069	8,534	6,649	0,931	1,754	4,038
13,871	6,935	10,914	0,841	1,879	4,327



Tabel pengaruh konsentrasi terhadap adsorpsi ion Cd(II) pada adsorben ALBM-Dtz

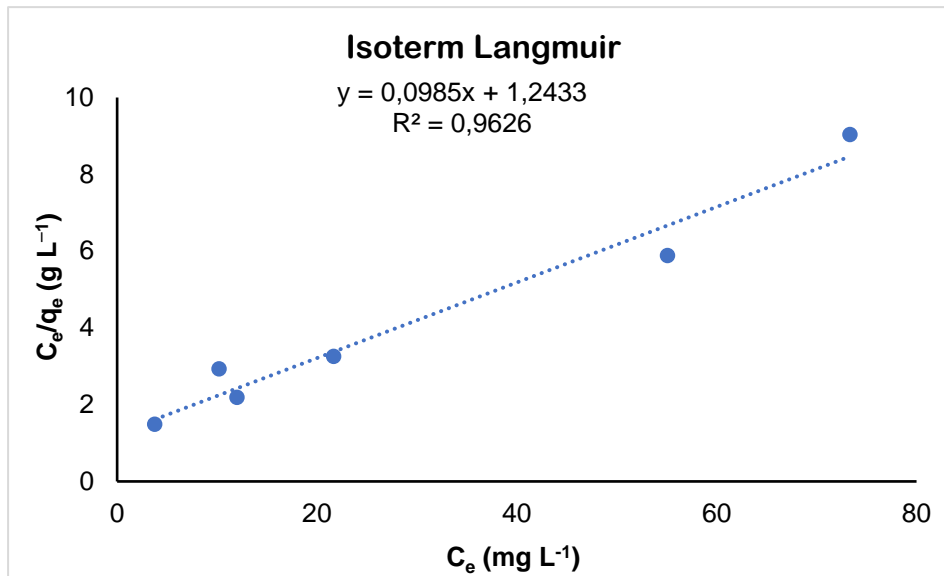
Konsentrasi	A_0	A_e	fp	C_0 (mg L ⁻¹)	C_e (mg L ⁻¹)
10	0,116	0,030	10	8,827	2,856
20	0,236	0,062	10	17,146	5,086
30	0,209	0,070	15	22,974	8,477
40	0,240	0,130	20	34,963	19,067
60	0,254	0,175	40	73,810	51,817
80	0,311	0,245	40	89,566	71,262

$C_0 - C_e$ (mg L ⁻¹)	q_e (mg g ⁻¹)	c_e/q_e	log q_e	log c_e	ln c_e
5,972	2,986	0,956	0,475	0,456	1,049
12,060	6,030	0,843	0,780	0,706	1,627
14,496	7,248	1,170	0,860	0,928	2,137
15,356	7,678	2,554	0,885	1,292	2,976
21,993	10,997	4,712	1,041	1,714	3,948
18,304	9,152	7,786	0,962	1,853	4,266



Lampiran 22 Persamaan isoterm adsorpsi

Persamaan isoterm langmuir untuk adsorpsi Cd(II) pada adsorben ALB-Akt



$$C_e/m = 1/b \cdot C_e + 1/(k \cdot b)$$

Jika diambil plot C_e/m lawan C_e maka akan dapat diperoleh garis lurus dengan nilai $1/q_e$ sebagai *slope* dan $1/(k \cdot b)$ sebagai intersep, sehingga:

Persamaan garis lurus:

$$Y = 0,0985x + 1,2433$$

$$R^2 = 0,9626$$

Maka

$$1/q_e = 0,0985$$

$$q_e = 10,152 \text{ mg g}^{-1}$$

$$1/(k_L \cdot (q_e)^2) = 1,2433$$

$$1/(k_L \cdot (10,152)^2) = 1,2433$$

$$k_L = 1930517 = 19,30 \times 10^5 \text{ L mol}^{-1}$$

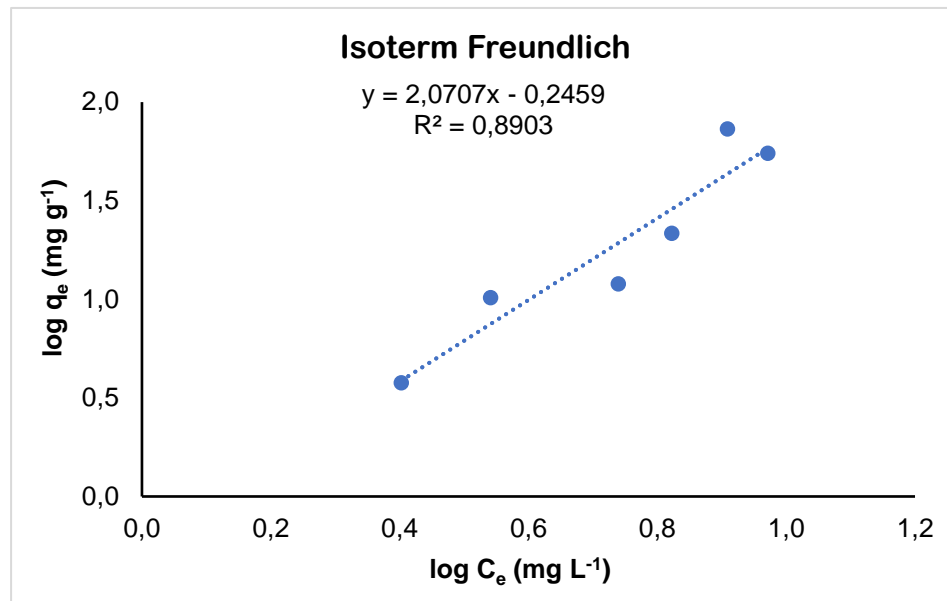
$$E = RT \ln k_L$$

$$= -8,314 \times 298 \times \ln 1930517$$

$$= -37552,11 \text{ J mol}^{-1}$$

$$= -37,552 \text{ kJ mol}^{-1}$$

Persamaan isoterm freundlich untuk adsorpsi Cd(II) pada adsorben ALB-Akt



$$\log q_e = \log k + 1/n \log C_e$$

Jika diambil plot $\log q_e$ lawan C_e maka akan dapat diperoleh garis lurus dengan nilai $1/n$ sebagai *slope* dan b sebagai intersep, sehingga :

Persamaan garis lurus:

$$Y = 2,0707x - 0,2459$$

$$R^2 = 0,8903$$

Maka

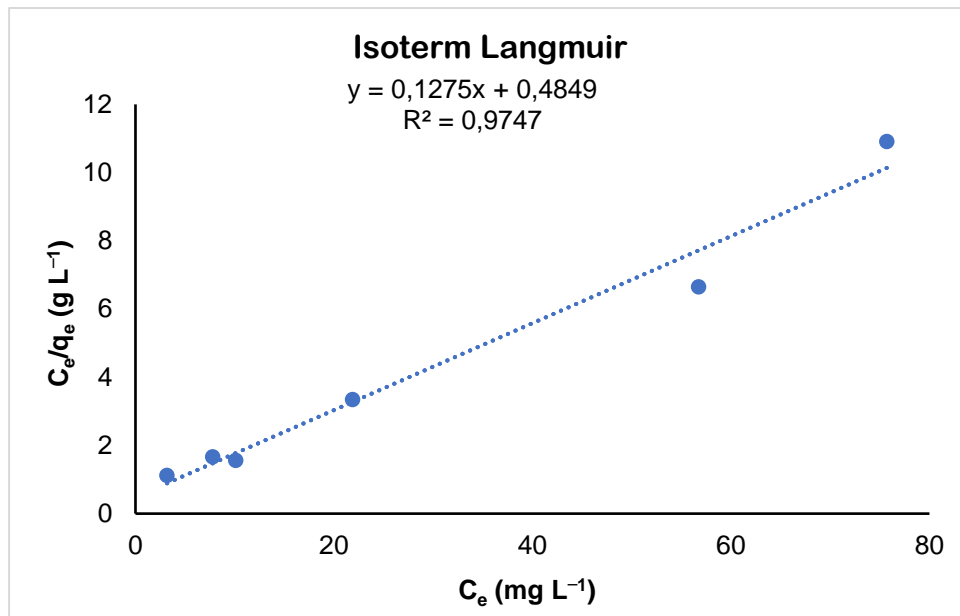
$$1/n = 2,0707$$

$$n = 0,48$$

$$\log k_F = -0,2459$$

$$k_F = 0,567 \text{ L mol}^{-1}$$

Persamaan isoterm langmuir untuk adsorpsi Cd(II) pada adsorben ALBM



$$C_e/m = 1/b \cdot C_e + 1/(k \cdot b)$$

Jika diambil plot C_e/m lawan C_e maka akan dapat diperoleh garis lurus dengan nilai $1/q_e$ sebagai *slope* dan $1/(k_L \cdot q_e)$ sebagai intersep, sehingga:

Persamaan garis lurus:

$$Y = 0,1275x + 0,4849$$

$$R^2 = 0,9747$$

Maka

$$1/q_e = 0,1275$$

$$q_e = 7,843 \text{ mg g}^{-1}$$

$$1/(k_L \cdot (q_e)^2) = 0,4849$$

$$1/(k_L \cdot (7,843)^2) = 0,4849$$

$$k_L = 3824048 = 38,24 \times 10^5 \text{ L mol}^{-1}$$

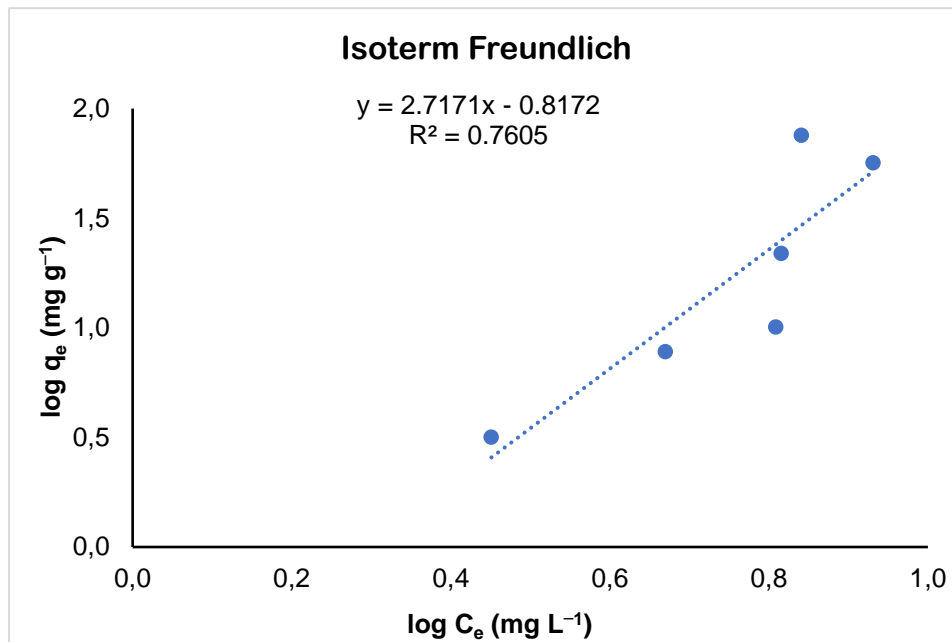
$$E = RT \ln k_L$$

$$= -8,314 \times 298 \times \ln 3824048$$

$$= -37552,112 \text{ J mol}^{-1}$$

$$= -37,552 \text{ kJ mol}^{-1}$$

Persamaan isoterm freundlich untuk adsorpsi Cd(II) pada adsorben ALBM



$$\log q_e = \log k + 1/n \log C_e$$

Jika diambil plot $\log q_e$ lawan C_e maka akan dapat diperoleh garis lurus dengan nilai $1/n$ sebagai *slope* dan b sebagai intersep, sehingga :

Persamaan garis lurus:

$$Y = 2,7171x - 0,8172$$

$$R^2 = 0,7605$$

Maka

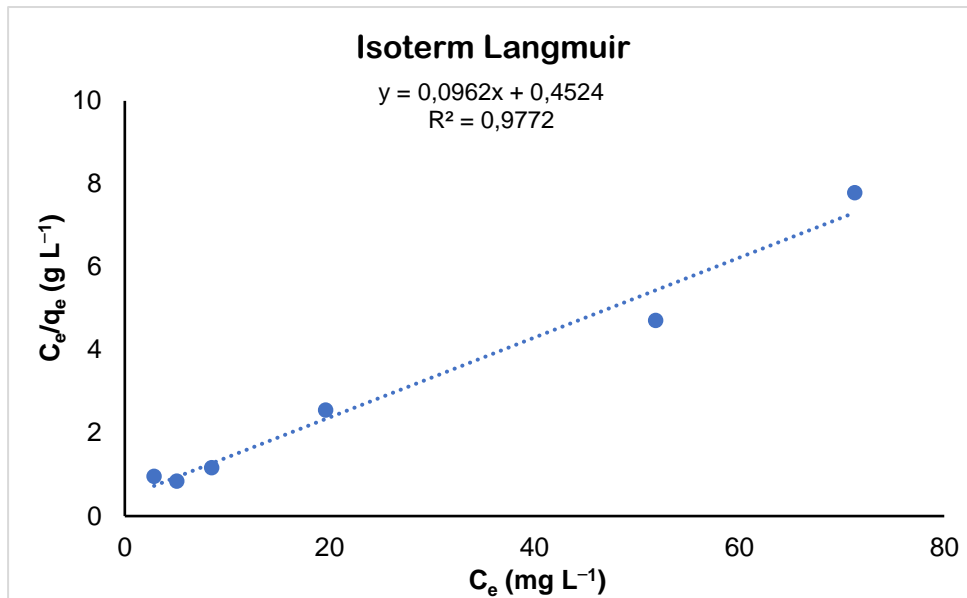
$$1/n = 2,7171$$

$$n = 0,368$$

$$\log k_F = -0,8172$$

$$k_F = 0,152 \text{ L mol}^{-1}$$

Persamaan isoterm langmuir untuk adsorpsi Cd(II) pada adsorben ALBM-Dtz



$$C_e/m = 1/b \cdot C_e + 1/(k \cdot b)$$

Jika diambil plot C_e/m lawan C_e maka akan dapat diperoleh garis lurus dengan nilai $1/q_e$ sebagai *slope* dan $1/(k_L \cdot q_e)$ sebagai intersep, sehingga:

Persamaan garis lurus:

$$Y = 0,0962x + 0,4524$$

$$R^2 = 0,9772$$

Maka

$$1/q_e = 0,0962$$

$$q_e = 10,395 \text{ mg g}^{-1}$$

$$1/(k_L(q_e)^2) = 0,9772$$

$$1/(k_L(10,395)^2) = 0,9772$$

$$k_L = 5432453 = 54,32 \times 10^5 \text{ L mol}^{-1}$$

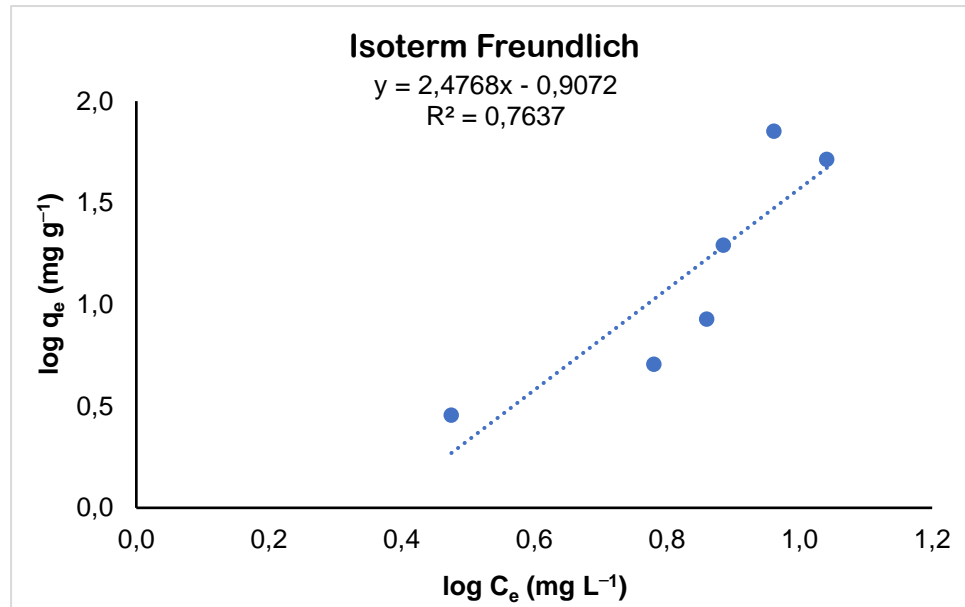
$$E = RT \ln k_L$$

$$= -8,314 \times 298 \times \ln 5432453$$

$$= 38421,896 \text{ J mol}^{-1}$$

$$= 38,422 \text{ kJ mol}^{-1}$$

Persamaan isoterm freundlich untuk adsorpsi Cd(II) pada adsorben ALBM-Dtz



$$\text{Log } q_e = \log k + 1/n \log C_e$$

Jika diambil plot Log q_e lawan C_e maka akan dapat diperoleh garis lurus dengan nilai $1/n$ sebagai *slope* dan b sebagai intersep, sehingga:

Persamaan garis lurus:

$$Y = 2,4768x - 0,9072$$

$$R^2 = 0,7637$$

Maka

$$1/n = 2,4768$$

$$n = 0,404$$

$$\log k_F = -0,9072$$

$$k_F = 0,124 \text{ L mol}^{-1}$$

Lampiran 23 Perhitungan desorpsi

Tabel Perhitungan desorpsi pada adsorben ALB-Akt

Larutan Pendesorpsi	A	C	fp	%Desorpsi
Kontrol Cd	0,258	2,024	30	
ALB-Akt	0,172	1,360	30	
Akuades	0,006	0,06	30	10,118
KNO ₃	0,014	0,128	30	19,288
NH ₂ OHHCl	0,030	0,254	30	38,308
Na ₂ EDTA	0,004	0,055	30	8,316
Total				76,032

Larutan Pendesorpsi	C _e	C _e *V	fp	%Relatif	(C ₀ -C)V
Kontrol Cd	60,729	1,214	30		0,3985
ALB-Akt	40,801	0,816	30		
Akuades	2,016	0,040	30	13,307	
KNO ₃	3,843	0,076	30	25,369	
NH ₂ OHHCl	7,634	0,152	30	50,384	
Na ₂ EDTA	1,657	0,033	30	10,93	
Total				100	

Tabel Perhitungan desorpsi pada adsorben ALBM

Larutan Pendesorpsi	A	C	fp	%Desorpsi
Kontrol Cd	0,258	2,024	30	
ALBM	0,176	1,386	30	
Akuades	0,003	0,040	30	6,421
KNO ₃	0,023	0,202	30	31,704
NH ₂ OHHCl	0,039	0,324	30	50,944
Na ₂ EDTA	0,021	0,181	10	9,487
Total				98,558

Larutan Pendesorpsi	C _e	C _e *V	fp	%Relatif	(C ₀ -C)V
Kontrol Cd	60,729	1,214	30		0,382
ALBM	41,599	0,819	30		
Akuades	1,228	0,024	30	6,515	
KNO ₃	6,065	0,121	30	32,168	
NH ₂ OHHCl	9,745	0,194	30	51,689	
Na ₂ EDTA	1,815	0,036	10	9,626	
Total				100	

Tabel Perhitungan desorpsi pada adsorben ALBM-Dtz

Larutan Pendesorpsi	A	C	fp	%Desorpsi
Kontrol Cd	0,258	2,024	30	
ALBM-Dtz	0,116	0,921	30	
Akuades	0,002	0,034	30	3,091
KNO ₃	0,028	0,238	30	21,578
NH ₂ OHHCl	0,082	0,660	30	59,842
Na ₂ EDTA	0,016	0,143	30	13,036
Total				97,549

Larutan Pendesorpsi	C _e	C _e *V	fp	%Relatif	(C ₀ -C)V
Kontrol Cd	60,729	1,214	30		0,6619
ALBM-Dtz	27,631	0,552	30		
Akuades	1,023	0,0204	30	3,169	
KNO ₃	7,142	0,142	30	22,121	
NH ₂ OHHCl	19,806	0,396	30	61,345	
Na ₂ EDTA	4,314	0,086	30	13,363	
Total				100	